Mémoire

Auteur : Meulders, Catherine
Promoteur(s) : Gregoire, Marilaure; Mouchet, Anne
Faculté : Faculté des Sciences
Diplôme : Master en océanographie, à finalité approfondie
Année académique : 2018-2019
URI/URL : http://hdl.handle.net/2268.2/8234

MODELLING NITROGEN DYNAMICS IN THE BLACK SEA

Author : Catherine MEULDERS

Supervisors : Marilaure GRÉGOIRE and Anne MOUCHET

A Thesis Submitted in Partial Fulfillment of the Requirements for the Master's Degree in Oceanography

University of Liège - Faculty of Sciences

Academic year 2018-2019

Conformément aux règles imposées à la rédaction, ce mémoire ne doit pas dépasser 50 pages, rédigées en Times 12 ou équivalent.

ACKNOWLEDGMENTS

I am particularly thankful to my two promoters. Firstly, I would like to thank Marilaure Grégoire, for having shaped this project around my center of interest. I also would like to thank her for the time spent to discuss some issues and explain new concepts. Many thanks to Anne Mouchet as well, who took the necessary time to teach me new tools that eventually will not be used in the frame of this work.

I also would like to thank all of the MAST's members, who welcomed me warmly.

Furthermore, I would like to express my gratitude to the members of the jury, who accepted to be part of this journey and for their respective reading.

Finally, I would like to express my sincere gratitude to my family, for their unconditional support.

I would like to specially mention my Dad, to whom this work is dedicated.

CONTENTS

Summary

La Mer Noire est considérée comme le plus grand bassin anoxique au monde avec pour conséquence de rapides variations du potentiel d'oxydo réduction des masses d'eau. Ces variations entraînent l'apparition de réactions comme la dénitrification et l'oxydation anaérobique de l'ammonium (anammox) qui influencent grandement la quantité d'azote fixé (principalement ammonium et nitrate) dans la Mer Noire. Les pertes d'azote liées à ces réactions sont possiblement compensées partiellement par l'apport des rivières, mais une autre source (fixation de l'azote par des micro-organismes dits "diazotrophes" - cyanobacteries ou bacteries heterotrophes) a été démontrée à plusieurs reprises. Elle est cependant difficilement quantifiable.

L'ajout de diazotrophes (cyanobacteries photo autotrophes) dans un modèle existant a permis de montrer que ces micro organismes ont un rôle à jouer dans le cycle de l'azote en Mer Noire et que, même si les taux calculés par le modèle sont inférieurs à ceux mesurés/calculés jusqu'à présent, ils compensent probablement une partie des pertes d'azote fixé. Il semble également important de poursuivre la démarche en ajoutant un second groupe de diazotrophes sous la forme de bactéries hétérotrophes.

The Black Sea is considered as the largest anoxic basin in the world, resulting in rapid variations of oxidation-reduction potential in the water column. These variations lead to the appearance of reactions such as denitrification and anaerobic oxidation of ammonium (anammox), which modify the content of fixed nitrogen (mainly ammonium and nitrate) in the Black Sea. The losses of nitrogen following these reactions are probably partially compensated by the inputs of rivers, but another source (nitrogen fixation by so-called "diazotrophic" microorganisms - cyanobacteria or heterotrophic bacteria) has been demonstrated several times. However, it is difficult to quantify. The addition of diazotrophs (photo autotrophic cyanobacteria) in an existing model has shown that these microorganisms have a role to play in the nitrogen cycle of the Black Sea and that, even if the rates calculated by the model are lower than those measures / calculated so far, they probably compensate for some of the fixed nitrogen losses. It also seems important to continue the process by adding a second group of diazotrophs in the form of heterotrophic bacteria.

CHAPTER 1

INTRODUCTION

1.1 Context and objectives of this master thesis

In a global warming world, ocean deoxygenation becomes a threat. The increasing temperature of both the air and the water not only decreases oxygen solubility but also strengthens the stratification and therefore limits dissolved oxygen supply to the ocean interior ([28], [13]). In coastal waters, this phenomenon can be due to a high use of fertilizers (eutrophication) ([2]). In this case, rivers bring both nitrogen and phosphorus in abundance enabling proliferation of marine life. The resulting significant levels of respiration of this organic matter lead to a high consumption of oxygen.

The depletion of dissolved oxygen content, whatever the main mechanism involved, has a strong impact on other biochemical cycles, including on the nitrogen cycle ([2]). Within the latter, denitrification (all of the chemical processes by which fixed nitrogen [1] is converted to dinitrogen (N_2)) occurs only in anoxic waters. The losses of fixed nitrogen are compensated mainly by nitrogen fixation, even if atmospheric deposition and continental runoffs have a role to play ([23], [22]). N_2 fixation is accomplished by N_2 fixers or diazotrophs.

Altogether, the marine nitrogen cycle is disrupted by the simultaneous threats of climate change (i.e. the resulting ocean deoxygenation) and eutrophication ([21]). The controlling mechanisms that link N loss and N2 fixation remain enigmatic and it is not yet known whether,

[1] NO_3^-, NO_2^-, NH_4^+, N_2O, PON and DON ([22])

on what time scales and to what extent global rates of N2 fixation respond to changes in N loss processes.

In this context, completing the nitrogen cycle of an existing model (BAMHBI) of the Black Sea (an anoxic basin for the most part) by adding diazotrophs seems important better constrain the nitrogen budget. This is the main purpose of this master thesis. To reach this goal, the model (1D column) is first parametrized without the N_2-fixers to match a typical water column of the Black Sea in the first part of the 21^{th} century. Then, the new planktonic group is added before performing a sensitivity analysis on the parameters.

1.2 The Black Sea

The Black Sea is an inland sea located between Eastern Europe and Western Asia (between 40°55' - 46°32'N and 27°27' - 41°32'E). While the basin is connected to the Azov Sea through the Kertch Strait to the north, its main connection with other water bodies lies in the south-west, where the Black Sea is linked to the Mediterranean Sea through the Bosphorus Strait (width: 0,36-3,6km; depth: $<$ 93m ([67]), the Marmara Sea and the Dardanelles Strait.
At basin-scale, the Black Sea circulation comprises two large cyclonic gyres surrounded by a cyclonic boundary current. The latest, known as the "Rim Current", is mainly created by wind stress and flows along the continental slope, by the topography of which it is also modified. Another specific feature of the Black Sea is the presence of the Cold Intermediate Layer (CIL). This notable water mass thickness varies from 25 m to 100 m (depending on the season) and is characterized by a temperature below 8° Celsius all year long and across the whole basin. During summer, the subsurface layer above the CIL can reach 25° C, while during winter, the lower boundary of it can be found under the lower boundary of the mixed layer ([42]). The deep water mass being at 9°C, the CIL is therefore the coldest layer of the Black Sea. As nutrients are transported by advection within this layer, it plays an important role in the supply and recycling of nutrients ([41]).

The Black Sea is an enclosed basin, thus having knowledge of the water balance is essential for the understanding of the mass budget of diverse chemical components. The Black Sea is a dilution basin in which the sum of runoffs and precipitation exceeds evaporation ([41]). The main river inputs come from the Danube (75% of all river inputs), the Dniepr and the Dniestr, all located in the north-western part of the sea. The Black Sea surface area (4.2 $10^5 km^2$) is

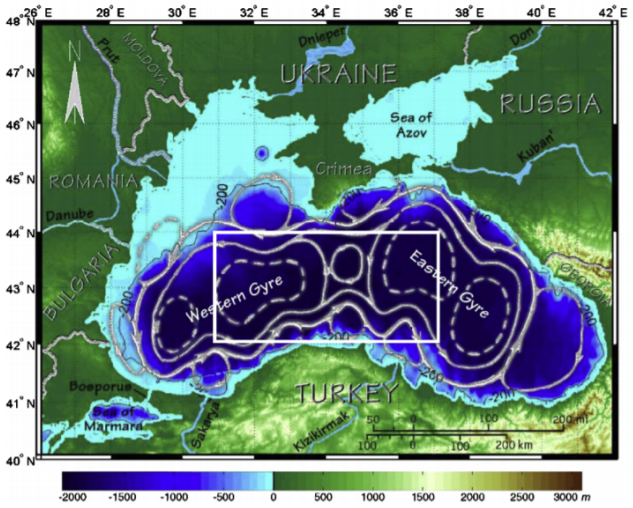

Figure 1.1: **The Black Sea geography, bottom topography and circulation (figure reproduced from Oguz et al. (1993) after modifications by Chu et al. (2005)). The model is considered to be representative of the situation in the central Black Sea which has been delimited as the region between 42–44N, 31–37E with a depth of 2000 m (in the rectangle). After Grégoire et al,2008 [18]**

five times smaller than the one of its catchment basin. The large size of the latter has a strong influence on nutrient loading and consequently on biota of the Black Sea, as it brings industrial, domestic, and agricultural runoffs of more than 162 million people ([41]). These large inputs of fresh water also play a major role in the strong stratification of the Black Sea. Indeed, due to these inputs, the surface salinity is around 18, while the deep inflowing Mediterranean water mass brings water with a salinity about 36 ([57]). The mean salinity of the basin below the surface mixed layer is itself around 22. As a result, a permanent pycnocline expands between densities between $\sigma_t \approx 14.5$ and 16.6 ([18]) and prevents mixing between surface and deep waters. One of the consequences of this lack of blending is that oxygen is rapidly and totally consumed by respiration of sinking organic matter ([57]). This explains why the Black Sea is known to be the world's largest anoxic basin ([67]).

The well oxygenated surface layer is most often about 50 m thick ([33]; [18]), but its thickness changes depending on the region taken into consideration. According to Yakushev et al.,2007, ([67]), it can vary from 70-100m in the central basin to 120-200m in the peripheral areas. It is separated from the sulfidic deep waters by a transition zone (the so-called 'suboxic layer'), which lies at a depth corresponding to densities between $\sigma_t \approx 15.6$ and 16.2 ([33]). Within this layer, both of oxygen and sulfide concentrations are very low, with no overlap ([67]) and a lot of redox processes (reduction of nitrate, manganese oxide or iron oxide) occur ([33]; [36]; [17]). As the downward flux of oxygen seems to be insufficient to suppress the upward

flux of sulfide, a lateral input of O_2 from the Bosporus is suspected. Finally, the deepest layer ($\sim 150 - 2000$m) is a sulfidic layer, which is also characterized by a high concentration of ammonium (up to 100 μM) ([36]). The thickness of the different layers is neither spatially nor temporally constant, but biochemical properties and chemical species follow precisely density (σ_t) (except in the Bosporus plume). Due to all these characteristics, the Black Sea is often considered as a site of choice to study anoxic marine environments ([37], [33], [31]).

1.3 The nitrogen cycle

1.3.1 Generalities

Nitrogen is a key component in life. It is needed by all living beings for the synthesis of both the genetic code and proteins.

On Earth and in the ocean, the nitrogen cycle enters in a large scale biogeochemical loop including, in addition to the oxygen cycle already mentioned, the carbon (C) and phosphorus (P) cycles (1.2). This imbrication of the different cycles is, by coupling physical and biochemical processes, fundamental for the Earth's climate ([22], [20]). The N cycle depends primarily on micro organisms that perform reduction-oxidation (redox) reactions. The long-term recycling through the geosphere also plays a role but that one is less important at scales of geologic times ([4]).

A. Nitrogen forms

In oceans, nitrogen can be found under various forms. The most abundant of them is the inert dissolved N_2 gas. Because of the high energy cost of breaking the triple bond $N \equiv N$, only few species are able to use N_2 as a source of nitrogen for growth. Bio-available forms of nitrogen (fixed nitrogen) are preferred, although they are much sparser and often limit primary production ([4]).

The marine nitrogen cycle is singular in the way it contains five nitrogen forms of relatively stable oxidation states ([20]) :

- NO_3^- (nitrate), oxidation state = +V,
- NO_2^- (nitrite), oxidation state = +III,
- N_2O^- (nitrous oxide), oxidation state = +I,

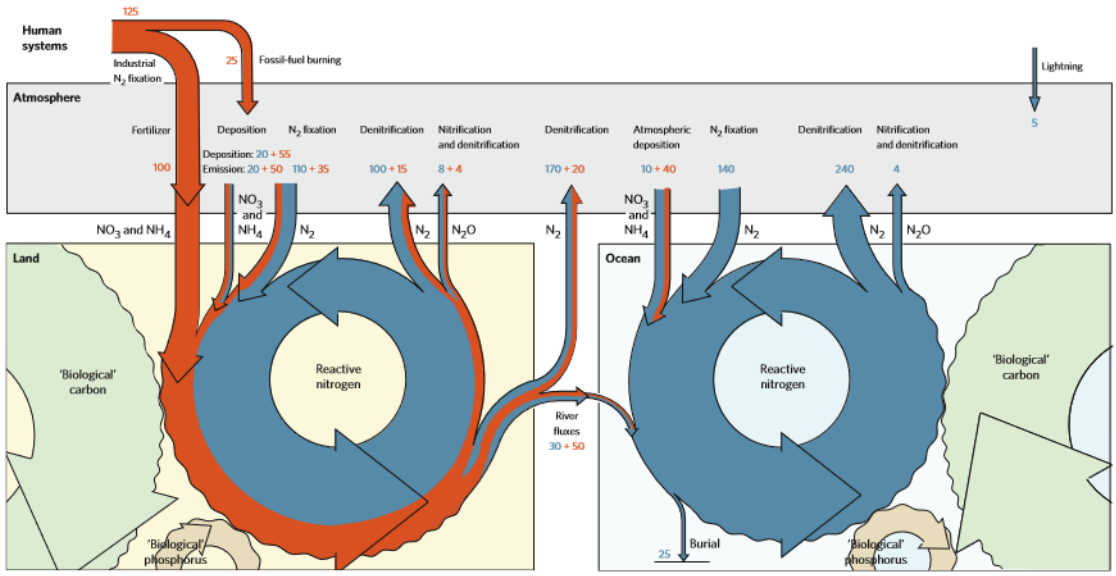

Figure 1.2: **Depiction of the global nitrogen cycle on land and in the ocean, showing the major processes that transform molecular nitrogen into fixed nitrogen (and back), and the tight coupling between the nitrogen cycles (land and ocean) with those of carbon and p. Blue fluxes = 'natural' (unperturbed) fluxes; orange fluxes = anthropogenic perturbation. Values (Tg N per year) are for the 1990s. Few of these flux estimates are known to better than ±20%, and many have uncertainties of ±50% and larger. After Gruber et al.,2008 ([22])**

- N_2 (molecular nitrogen), oxidation state = 0,
- NH_4^+ (ammonia) and amino-acids, oxidation state = -III

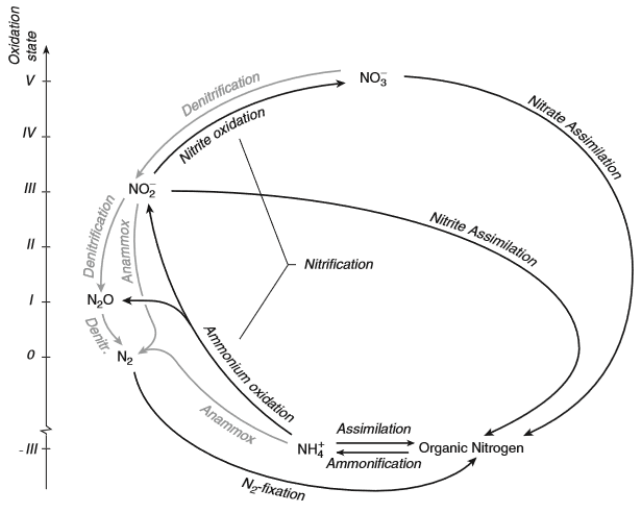

Figure 1.3: **Major chemical forms and transformations of nitrogen in the marine environment. The various chemical forms of nitrogen are plotted versus their oxidation state. Processes shown in grey occur in anoxic environments only. After Gruber, 2008 ([20])**

By generating N_2O through nitrification (by-product) or denitrification (intermediate product), the marine environment contributes to global warming to a certain extend. Indeed, N_2O is

a potent greenhouse gas ([4]).

Several reactions exist to shift from one oxidation state to another (1.3). Different kind of phytoplankton or bacteria are able to perform one or several of these reactions to transform nitrogen in a molecule at the lowest oxidation state and meet their need for nitrogen. However, the bigger the oxidation state of the starting molecule, the more energy it requires to perform the reaction (except for N_2, as the triple bond requires even more energy to be broken).

B. Reactions

The different reactions carried out by marine micro organisms can be divided in four main processes : assimilation, remineralization of organic matter, losses of fixed nitrogen in the water column and dinitrogen fixation.

Assimilation Most of phytoplankton and bacteria can assimilate either nitrate or ammonium to turn it into organic nitrogen. If NH_4 is present, its assimilation will be privileged as no redox reaction is required. Nevertheless, nitrate reductase is present in almost all phytoplankton since $NO_3{}^-$ is much more abundant than NH_4 in a lot of places ([20]).

Regeneration of organic matter The opposite processes of assimilation include remineralization (ammonification) and nitrification. Most of organic matter is remineralized by ammonification. This reaction leads to transformation of organic nitrogen into $NH_4{}^+$ or NH_3. It can be performed by bacteria (hydrolysis) and zooplancton (excretion) in both oxic or anoxic conditions.

The second way to regenerate organic matter is nitrification. Two successive reactions are required to complete the process ($NH_4{}^+$ oxidation and $NO_2{}^-$ oxidation). Both of them must take place in aerobic condition and are made solely by chemo-autotrophic bacteria (Nitrosomonas and Nitrobacter respectively). They use the energy from these reactions to fix inorganic carbon in the dark ([4]), and the whole process can be inhibited by light ([52]).

Losses of fixed nitrogen in the water column In the absence of oxygen, $NO_3{}^-$ can be used as an electron acceptor for micro organisms ([4]) through two main processes that are denitrification and anaerobic ammonium oxidation (anammox). Both lead to the formation of N_2, permanently removing fixed nitrogen from the water column ([12], [11],[33], [15], [64]).

Denitrifiers can be either autotrophic or heterotrophic microbes and convert $NO_3{}^-$ into N_2 following several steps:

$$NO_3{}^- \rightarrow NO_2{}^- \rightarrow N_2O \rightarrow N_2$$

In the process, denitrifiers consume organic matter and therefore also regenerate other inorganic nutrients (CO_2, $PO_4{}^{3-}$) ([64]).

Bacteria which perform anammox reaction are compulsorily both autotrophic and anaerobic. In this process, $NH_4{}^+$ and $NO_2{}^-$ are combined to produce N_2. Consequently, they highly depend on the local concentration of those two species and must be close to areas where ammonification and nitrification and/or denitrification take place.

According to Ward et al.,2009 ([64]), both processes are observed in areas depleted in oxygen across the world, but the ratio between those two mechanisms can vary spacially a lot. On the contrary, Canfield et al.,2010 ([4]), mentions that N_2 production in many marine environment comes mainly from anammox reaction.

N_2 fixation On the contrary, a major source of fixed nitrogen in the ocean is N_2 fixation ([22], [38]). The exact magnitude as well as the spatial and temporal distribution of N_2 fixation remain difficult to evaluate ([11]), partly due to a lack of experimental data coverage ([60]). Moreover, mechanisms controlling marine N_2 fixation are not well understood ([38]). Micro organisms that convert N_2 into organic nitrogen can be both photo autotrophic cyanobacteria or heterotrophic bacteria. Some are unicellular, while others live in colonies or in symbiosis within some species of diatoms ([20]). They can live in a wide range of different environments, from euphotic and oxygenated waters to aphotic areas or oxygen deficient zones ([38], [30]). Although several species of cyanobacteria are able to use N_2 as a source of nitrogen, *Trichodesmium sp.* is believed to be the most significant N_2 fixer in the open ocean ([25], [47]) and is often used in modeling autotrophic dinitrogen fixers in the ocean.

To estimate whether N_2 fixation happens in a given water body, tools for either field experiments or modelling have been created. If water samplings are available, both isotopic or genetic analyses can be carried out in order to check whether N_2 fixation (isotopic) or N_2 fixers (genetic) are present. For example, a protocol described by Montoya ([43]) allows direct measurements of N_2 fixation using high sensitivity isotope ratio mass spectrometer while the presence of an essential gene (*nifH*) for diazotrophs can reveal these organisms in the sampled water.

In modelling, two conservative tracers N^* and P^* have been used for several years to spot areas where diazotrophs could thrive. The first one, N^*, has been defined by Gruber ([23]) and investigates the spatial distribution of N_2 fixation and denitrification in the world oceans. By definition, $N^* = N - r_{nitr}^{N:P}P + constant$, where $r_{nitr}^{N:P}$ is the stoechiometric ratio during the remineralization of organic material while the constant must be determined. On a whole, the idea is to have an easy diagnostic to account for denitrification and N_2 fixation only, removing the effect of regeneration of organic matter. The absolute value of N^* can be indicative of denitrification (negative values) or N_2 fixation (positive) although only the change in N^* from a conservative behaviour can be interpreted as a net effect of denitrification or N_2 fixation ([23]). Similarly, Deutsch ([11]) proposed a second tracer, $P^* = (PO_4)^{3-} - NO_3{}^-/16$, to monitor the phosphate excess and spot the potential niche of nitrogen fixers. Based on the assumption that a constant N:P ratio of 16:1 is due to the biological uptake and remineralization by non-diazotrophic plankton, a decrease in P^* is expected in presence of N_2 fixers. Indeed, non-diazotrophic phytoplankton will consume N and P in a ratio close to the Redfield ratio, while N_2 fixers will consume proportionally more phosphorus.

1.3.2 The nitrogen cycle in the Black Sea

In the Black Sea, the concentration of inorganic nitrogen varies both temporally and spatially within the upper layer. This results from the successive phytoplankton blooms throughout the year, from the influence of rivers inputs near the coasts and from the presence of denitrification and anammoxs that has been shown several times in the redox zone of the basin ([36], [15], [26]). As chemical compounds are found at a depth that follows precisely density (σ_t), the following mentions of 'depth - σ_θ' will refer to the depth at which this density is found.

A. Nitrogen forms

Ammonium and ammonia Unlike what happens in other oceans and seas in the world, the deep basin of the Black Sea contains 98% of the total inorganic nitrogen stock in the form of NH_4^+ (instead of NO_3^- elsewhere). This phenomenon comes from the combination of the lack of nitrification in deep waters (accumulation of $NH_4{}^+$) and denitrification that prevent $NO_3{}_-$ formation ([67]). At the surface, the concentration of ammonium is very weak (between 0.2µM in summer and 0.4µM in winter) and begins to increase only at a depth of $\sigma_\theta = 15.90 - 16.00$ kg m^{-3}. Its maximum concentration (around 90 μM) is reached at depth.

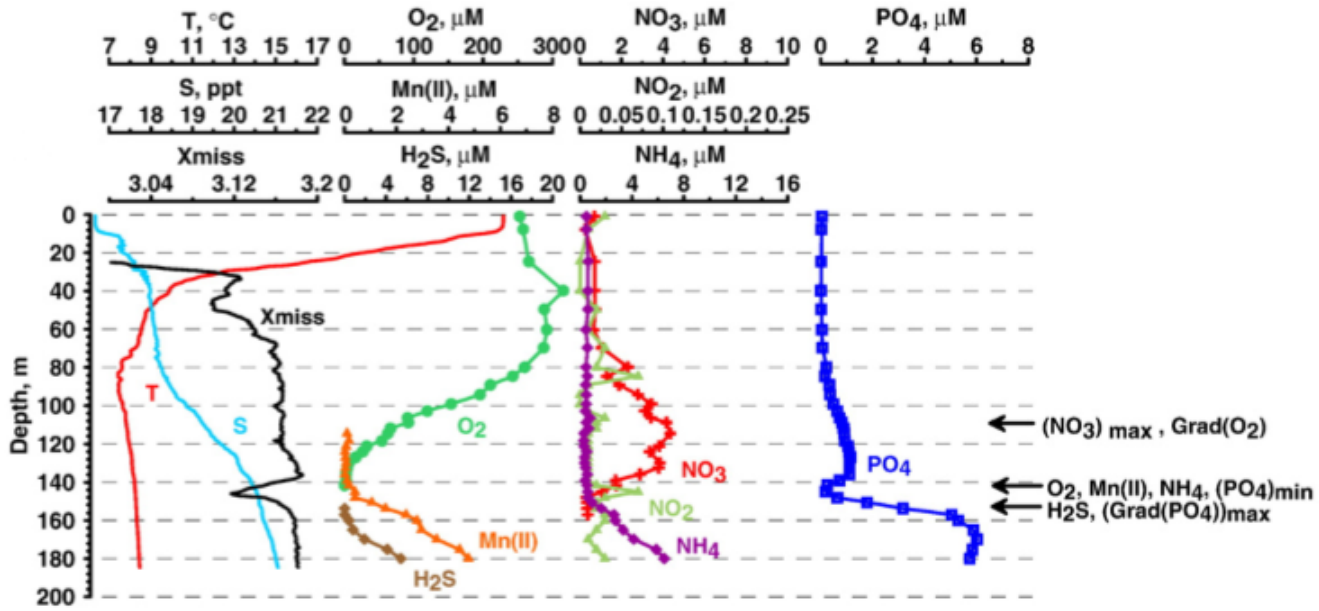

Figure 1.4: **Vertical distributions of hydrochemical parameters in the Black Sea. "Xmiss" corresponds to Dr Haardt, turbidity data. The arrows show the depths of: (1) NO_3 maximum and the lower portion of the oxycline; (2) O_2 depletion, the onsets of Mn(II) and NH_4, and the PO_4 minimum; and (3) the onset of H_2S and the maximum PO_4 gradient. After [66]**

Nitrate and nitrite As what is observed for ammonia, surface nitrate concentrations also vary throughout the year from less than 1µM in summer to 4 to 6 µM in winter depending on its consumption by phytoplankton. Deeper but still in the oxic layer, NO_3^- is produced by nitrification ([33]). Its maximum concentration (3-10 µM) is reached at a density equivalent depth comprised between $\sigma_\theta = 15.30 - 15.50$, before completely disappearing at a depth of $\sigma_\theta = 15.90 - 16.00$. Nitrate becomes the main oxidizing agent in the lower part of the redox layer and its massive consumption for denitrification and reduction by thiosulfate, elemental sulfur and sulfide explains its decrease below $\sigma_\theta = 15.30 - 15.50$.

Nitrite maximum concentrations lie between 0.02µM and 0.3µM ($\sigma_\theta = 15.90 - 16.00$), while there is always less than 0.1µM at the surface. The maximum of nitrite concentration is within a thin layer of water (less than 5m) and thus shows more spatial and temporal variability than other compounds.

Nitrous oxide Westley et al. ([65]) showed that N_2O does not accumulate in the Black Sea as it does in other low-O_2 environments. Moreover, the isotopic composition of N_2O does not match the one of other places studied. They explained these observations by an unusual combination of ammonium oxidation by nitrifiers and denitrification. However they did not

exclude the role of other reactions such as a coupling between the nitrogen and manganese redox cycles.

Nitrogen gas In 2008, both Fuchsman et al. ([15]) and Konovalov et al. ([33]) found that deep anoxic waters are supersaturated regarding N_2 in the Black Sea, while the maximum concentration is reached at the same depth as the peak of anammox ($\sim \sigma_\theta 16$).

B. Reactions

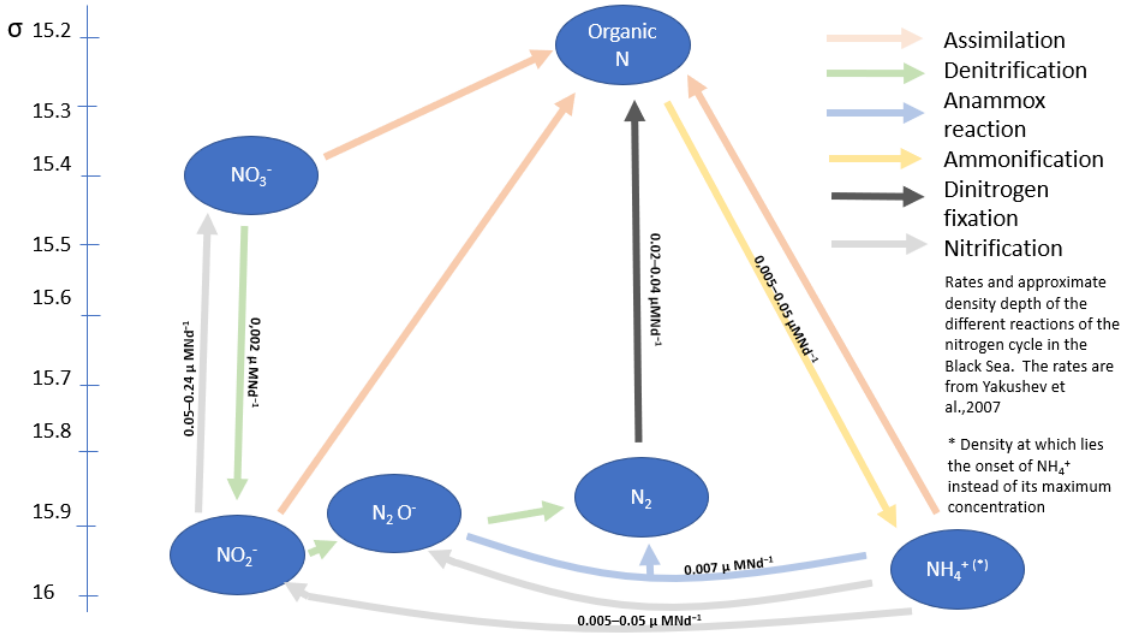

Figure 1.5: **Nitrogen species, main reactions and rates - approximately at the density of their maximum**

Nitrification : $NH_4^+ + 2O_2 \rightarrow NO_3^- + H_2O + 2H^+$ (after Konovalov ([33]))
By this process, ammonium is converted into NO_3^- between the lower part of the euphotic zone and the upper part of the suboxic zone. The presence of nitrifiers explains both the peaks of nitrate (final product) and nitrite (intermediate product) ([15], [41]). According to McCarthy ([41]), 80% of the NO_3^- taken up by phytoplankton derives from nitrification. However, the estimated rate of this reaction varies depending on the studies. The calculation can be done by inferring measures of NO_2^- production. Based on NO_2^- production, McCarthy [41] determined a nitrification rate of about 1.3 mmol N m^{-2} d^{-1} and compared it to the 0.29 mmol N m^{-2} d^{-1} found by Ward and Kilpatrick in 1991 (McCarthy integrated their values) and the 2.4 mmol N

m^{-2} d^{-1} that Yakushev and Neretin modelled in 1997. Both Gregoire ([19]) and Konovalov ([34]) computed similar values as MacCarthy (1,23 mmol N m^{-2} d^{-1} and 1 mmol N m^{-2} d^{-1} respectively), while Lam ([37]) found a rate of nitrification of 10 nM per day at 78m, which is within the range given by Ward and Kilpatrick ([37]).

Denitrification and ANAMMOX

Denitrification : $5(CH_2O)_{106}(NH_4)_{16}(PO_4) + 424NO_3^- + 424H^+ \rightarrow 530CO_2 + 5(PO_4) + 80(NH_4) + 212N_2 + 742H_2O$
Anammox : $5NH_4^+ + 3NO_3^- \rightarrow 4N_2 + 9H_2O + 2H^+$ (after Konovalov ([33]))

Denitrification and anammox are highly important in the nitrogen cycle of the Black Sea. These reactions are only possible under anoxic but non-sulfidic conditions, which explains the maximum N_2 concentration at the bottom of the suboxic layer ([33]). Several studies showed that anammox rate is more important than denitrification ([33], [37]), as N_2 production is mainly due to anammox (96% according to Konovalov), while the remaining 4% is made from denitrification (3%) and thio denitrification (1%). In 1991, Ward and Kirlpatrick found a rate of denitrification at 0.002 μM N d^{-1} ([66]) where Yakushev ([66]) modelled a rate 10 times higher.

Following the experiments conducted by Jensen ([26]), the anammox rate is 11.1 nM N d^{-1} at the maximum . The process is completely inhibited at a concentration of O_2 of 13.5 μM O_2. Kuypers ([36]) modelled a rate about 0 ,007 μM N d^{-1}, while Yakushev ([66]) found values of 0 – 0,03 μM N d^{-1}.

N_2 fixation In the Black Sea, direct and indirect evidences of N_2 fixation have been found. Kirkpatrick ([30]), using mRNA and stable isotops of nitrate to search for N_2 fixation, discovered chemobacteria that perform N_2 fixation in the suboxic waters as well as in the upper part of the sulfidic layer. He did not found any evidence of its presence in the euphotic zone. Presence of chemoautotrophs N_2 fixers had already been reported by Pshenin who isolated several strains (*Azotobacter, Clostridium, Pseudomonas, Vibrio, Spirillum* and *Treponema*) (Pshenin 1965, 1966, 1978 and 1980, as cited by [41]).

McCarthy ([41]) measured N_2 fixation rates in both the euphotic and aphotic zones thanks to an isotopic methodology. In 1999, N_2 fixation rates were measured in the euphotic zone only at two stations, at maximum values of 75 nmol N $kg^{-1}d^{-1}$. Two years later, he observed N_2

fixation in the aphotic zone alone and at lower maximum rates (54 nmol N $kg^{-1}d^{-1}$).

Applying an isotopic δ^{15} N distribution method as well, Fuchsman ([15]) calculated N_2 fixation rates of $\sim$150 nmol N $kg^{-1}d^{-1}$ which are twice as large as those found by McCarthy. Sorokin in 2002 found a rate of about 20-40 nmol N $kg^{-1}d^{-1}$ (given by [66]).

In the same experiment, she also showed inter annual variability in the fixation rates of N_2, as did Konovalov ([33]). The two of them reached the same conclusion that changes in the export of particulate organic nitrogen (PON) is probably an important factor. As N_2 fixers use preferentially light N_2 molecules as a source of energy (^{14}N), they favor the production of depleted δ^{15} N - PON resulting after remineralization in low δ^{15}N-NH_4. They modelled the relative use of

- the low δ^{15}N-NH_4 (δ^{15}N = -2 $^0/_{00}$) from N_2 fixers
- the high δ^{15}N-NH_4 (δ^{15}N= 5-7 $^0/_{00}$) from the deep sea

by anammox/denitrifiers and found that the diminution of δ^{15}N-N_2 due to remineralization of light PON generates a higher production and concentration of light N_2. They subsequently made the hypothesis that depleted δ^{15} N-PON from N_2 fixers determines the variability of lighter N_2 produced by anammox and denitrification reactions.

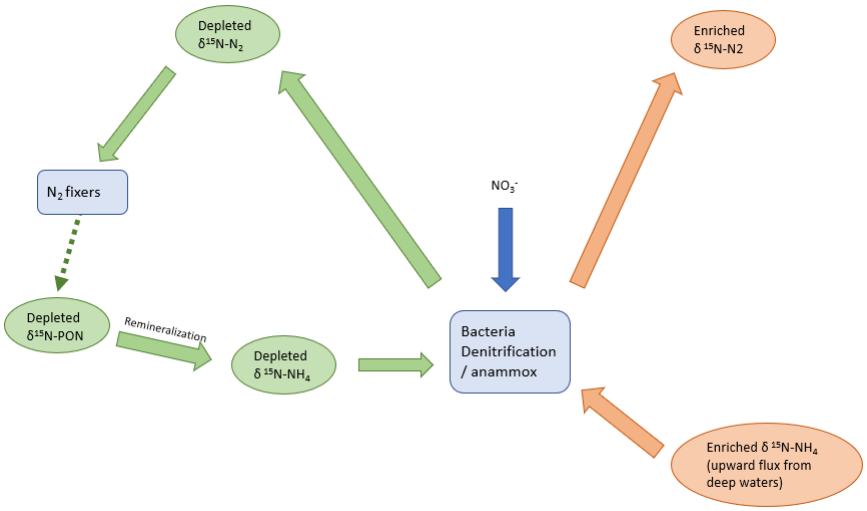

Figure 1.6: **Schematic explanation for the inter annual variability according to Konovalov ([33]) and Fuchsman ([15])**

The North Atlantic Oscillation (NAO) could also play a role, as it is known to impact the physical parameters, rates and biological reservoirs of the Black Sea on a decadal scale ([15], [33]).

CHAPTER 2

MATERIAL AND METHODS

2.1 The model

The model used in this master thesis is the coupled model BAMHBI-NEMO. The biogeochemical state variables are incorporated in the Biogeochemical Model for Hypoxic and Benthic Influenced areas (BAMHBI) while the Nucleus for European Modelling of the Ocean (NEMO) contributes to their evolution regarding physical characteristics.

In order to take into account specificities of each group, some changes have been made in the Chl:N ratio parameters. An accurate estimate of Chl:C ratio can better predict the phytoplankton biomass ([1], [40]). In addition to varying between species, this ratio is also influenced by light, temperature and nutrients ([61], [1],[40]). Sathyendranath ([49]) studied these ratio for several species of phytoplankton in offshore areas (NW Atlantic and Arabian Sea) and in the Bay of Tokyo. According to their results, diatoms and dinoflagellates have a similar range of Chl:C ratio, while Prymnesiophytes (coccolithophorite) shows a bigger ratio. The range of Chl:C (and then Chl:N) is taken from Sathyendranath ([49]) to take the inter species variability into account.

2.1.1 The hydrodynamical model : NEMO

The vertical distribution of the biochemical variables depends on physical parameters such as temperature, salinity, light penetration and mixing (advection being neglected in a 1D frame).

Over time, BAMHBI has been coupled to different hydrodynamics models (General Ocean Turbulence Model - GOTM, GHER3D and Nucleus for European Modelling of the Ocean - NEMO) to provide these elements. NEMO being the one now in use in the CMEMS (Copernicus Marine Environment Service) - Black Sea Monitoring and Forecasting Centre (BS-MFC) project is consequently the chosen physical model in this work.

2.1.2 The biogeochemical model : BAMHBI

A. Generalities

BAMHBI was first created in 1D ([18]) but now runs in 3D as well. It contains 28 state variables that allow the description of biological processes (bacteria, three groups of phytoplankton, two of zooplankton and two of gelatinous zooplankton) and chemical processes (simulation of oxygen, nitrogen, silicate and carbon cycles). Similarly to the modelling of diagenetic processes, one state variable (ODU) encompasses all the reduced molecules. The presence of the ODU allows the full coupling of processes that happen in the upper oxygenated layer and those in the anoxic deep layer ([18], [59]).
The model contains an additional benthic module that can represent processes of diagenesis ([5]) but that part will not be used in the frame of this work. The whole model is described in Gregoire et al. ([18]), except for the diagenesis part that can be found in Capet et al. ([5]). A description of all state variables (containing the new ones) is available in the Appendix 4.

As the Black Sea is deprived of oxygen below $\sim$ 100m, the model is tuned to explicitly represent processes linked to low oxygen environments (denitrification, anammox reactions). More particularly, in the current version of BAMHBI, inorganic nitrogen is modelled through two state variables NHS (lumping ammonium and ammonia) and NOS (lumping nitrate and nitrite). NOS is consumed by phytoplankton uptake denitrification, oxidation of ammonium and ODU and is produced by nitrification. Production of NHS depends on its excretion by bacteria, phytoplankton and zooplankton (NHS) while it is consumed by phytoplankton and bacteria uptake, anammox and nitrification (2.1. Moreover, since the exported material below 150m is definitely lost for the upper layer ecosystem, the amount of nitrogen loss in the form of particulate organic form is also compensated by a lateral export.

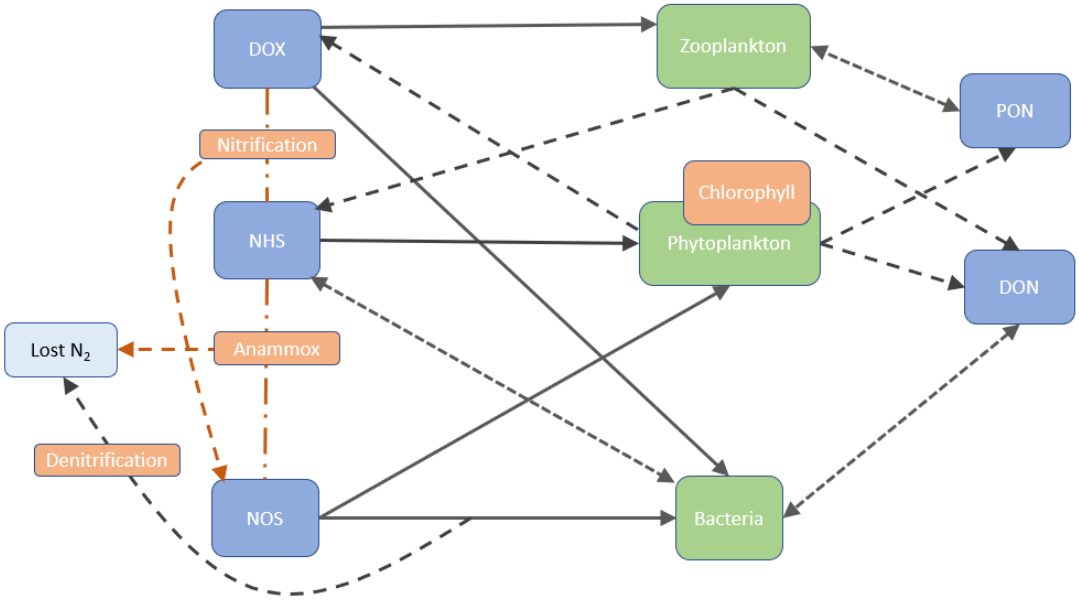

CHEMICAL STATE VARIABLES	DON	Dissolved organic nitrogen (encompasses labile and semi labile dissolved N)			
	PON	Particulate organic nitrogen			
	DOX	Dissolved oxygen			
	NHS	Ammonium + Ammonia			
	NOS	Nitrate + Nitrite			
BIOLOGICAL STATE VARIABLES	Bacteria	Bacteria			
	Zooplankton	Meso zooplankton + micro zooplankton + noctiluca + gelatinous			
	Phytoplankton	Diatoms + Flagellates + Emiliana			
CALCULATED OUTPUTS		Anammox	Denitrification	Nitrification	Chlorophyll
: biological reactions		: uptake by variable		: uptake and/or release	
: chemical reactions		: released by variable		: combination of 2 molecules	

Figure 2.1: **Schematic simplified representation of the nitrogen cycle in BAMHBI**

B. Parameters adaptation compared to the 3D version

Before adding new variables in the model, some changes in the parameters, justified by differences in physics between 3D and 1D models, are made to allow the model to reach a steady state typical of the 2010^{th}.

Parameter	3D	1D	Units	Justification - parameter description
Inhibition constants - ratio				Original values - after Gregoire [18]
kinanoxremdox	0,0005	0,005	-	Inhib. const. for O_2 inhib. anoxic respiration
kinanoxremnos	0,0005	0,005	-	Inhib. const. for NOS inhib. anoxic respiration
NOsNHsr	0,0	0,6	-	Mol NOs needed to oxidize 1 mol of NHs
Bacteria				To prevent their disappearance after 1 year
max growth rate	13,3	15,3	d^{-1}	maximum growth rate
mortality	0,05	0,04	d^{-1}	Mortality rate
growth efficiency	0,17	0,217	-	growth efficiency
Diatoms				To prevent their disappearance after 1 year
Min sinking rate	0,5	0,05	d^{-1}	Minimum sinking rate
Max sinking rate	2	0,5	d^{-1}	Maximum sinking rate
Predation on diatoms				Decreased to allow bloom of diatoms
Capt eff MesoZoo Diat	1	0,8	-	Capture efficiency of mesozooplankton on diatoms
Max grazing rate mesozoo	1,2	1	d^{-1}	Maximum grazing rate mesozooplankton
Redistribution				To obtain a constant N budget
k redistribute	57	37	layer	Layer at which the material is taken to be redistributed
Redistribute bottom flux top	5	100	m	Depth over which the material is redistributed (section 2.3.C)

Table 2.1: Modified parameters between BAMHBI-NEMO 3D and 1D

Later, a new species (N_2 fixers) is introduced in the model (see next section) and more parameters need to be changed to account for interspecies competition and prevent one group from disappearing or taking over the others. The following table shows only the parameters already present in the 3D model.

Parameter	3D	1D	Units	Justification
Phytoplankton				Competition for nutrient
NOS max uptake Flagellates	0,5	0,05	d^{-1}	Max NOs uptake rate
NHS max uptake Diatoms	0,5	0,05	d^{-1}	Max NHs uptake rate
ks NOS Flagellates	3,0	1,5	-	Half-sat const. for NOS uptake
ks NHS Flagellates	3,0	1,0	-	Half-sat const. for NHS uptake
ks NHS Diatoms	1,0	1,5	-	Half-sat const. for NHS uptake
ks PO_4 Flagellates	0,2	0,1	-	Half-sat const. for PO_4 uptake
ks PO_4 Diatoms	0,1	0,15	-	Half-sat const. for PO_4 uptake
Phytoplankton				Competition for light [1]
αPI Flagellates	0,2153	0,007153	d^{-1}	Half-sat light intensity
αPI Emiliana	0,3	0,035	d^{-1}	Half-sat light intensity
αPI Diatoms	0,3312	0,173312	d^{-1}	Half-sat light intensity
μ Max Flagellates	1	3	d^{-1}	Max. growth rate
μ Max Emiliana	2,5	2	d^{-1}	Max. growth rate
μ Max Diatoms	3,5	4	d^{-1}	Max. growth rate
Phytoplankton				Parameters linked to growth and mortality
Q10 PHY	2	1,6		after [51]
Q10 Diatoms	1.8	1,6		after [51]
Mortality Flagellates	0,03	0,003	d^{-1}	Mortality rate
Max grazing rate Microzoo	3,6	2,8	d^{-1}	Maximum grazing rate of microzooplankton
Capt eff MicroZoo Emiliana	1	0,7	-	Capture efficiency of microzooplankton on Emiliana
Capt eff MesoZoo Flagellates	0,4	0,1	-	Capture efficiency of mesozooplankton on Flagellates
Capt eff MesoZoo Emiliana	0,4	0,5	-	Capture efficiency of mesozooplankton on Emiliana

Table 2.2: Modified parameters between BAMHBI-NEMO 3D and 1D after addition of a new species

[1] : Note :light limitation depends on a decreasing exponential of $\frac{light * \alpha PI}{\mu Max}$

New parameters are listed in Appendix 4

C. Addition of diazotrophs

To our knowledge, several studies and models attempt to quantify the magnitude of N_2 fixation in the Black Sea ([41],[33] [66], [15]) but no biogeochemical model has an explicit representation of diazotrophs. The extension of the current modelled nitrogen cycle with N_2 fixers or diazotrophs is expected to enable a better understanding of the link between losses and production of fixed nitrogen in the Black Sea.

To simulate N_2 fixation, a new functional group of plankton, called diazotrophs, is added to the model through two state variables (CDZ - carbon diazotrophs and NDZ - nitrogen diazotrophs). This group accounts for a species of cyanobacteria (*Trichodesmium sp.*) which needs specific nutrients and light to grow. Their representation is therefore similar to that of the other groups of phytoplankton in the model but takes into account their own specificities. Only the differences between N_2 fixers and other groups of phytoplankton are listed here. The reader may refer to Gregoire[18] for the complete description of the photo-autotrophs.

The growth of diazotrophs is controlled by the uptake of nutrients and by light. Although iron is considered as a limiting nutrient for diazotrophs, we consider here that there is always enough Fe in the Black Sea environment. The large river inputs, dust deposition and iron concentration seem to justify this hypothesis. $(PO_4)^{3-}$ is then the only limiting nutrient and will determine the necessary uptake of fixed N rate to take up $(PO_4)^{3-}$. As what is described in the literature ([47], [45], [44]), diazotrophs favor the uptake of nitrate or ammonium when available but are able to switch to N_2 as a main source of nitrogen when the two other species are lacking. This behaviour minimizes the high energy cost of breaking the N_2 triple bond ([45]). Therefore, an extra parameter of respiration (DFixDiaz) is added to account for this increase in energy need with additional consumption of O_2 and an increased production of CO_2.

Then, two situations are considered. Either there is enough nitrate and ammonium in the environment to meet the need in fixed nitrogen and there is no need to perform N_2 fixation or the amount of fixed nitrogen is insufficient and uptake of N_2 is mandatory for the organisms to grow and respiration increases.

In accordance with Paulsen ([45]), grazing of diazotrophs by zooplankton is omitted. Indeed, observations seem to indicate that the grazing on *Trichodesmium sp.* is small ([45]). Natural mortality is the only sink term.

Growth rate

$$\frac{dCDZ}{dt} = \frac{\partial}{\partial z}(\tilde{\lambda}\frac{\partial CDZ}{\partial z}) + NetPhotosynthesis - (Respiration_{\mathrm{N_2}fixation} * DFixDiaz)$$
$$- CMortality - CLeakage$$
$$\frac{dNDZ}{dt} = \frac{\partial}{\partial z}(\tilde{\lambda}\frac{\partial NDZ}{\partial z}) + (\mathrm{NO}_s{}^{\mathrm{uptake}} + \mathrm{NH}_s{}^{\mathrm{uptake}} + \mathrm{N_2}{}^{\mathrm{uptake}}) - NMortality - NLeakage$$

Nutrient uptake if $\mathrm{NH}_s{}^{\mathrm{uptake}} + \mathrm{NO}_s{}^{\mathrm{uptake}} > \frac{\mathrm{P}^{\mathrm{uptake}}}{PNRedfield_{diaz}}$,
$\mathrm{N_2}{}^{\mathrm{uptake}} = 0$, otherwise :

$$\mathrm{NO}_s{}^{\mathrm{uptake}} = \mathrm{NO}umax * f^T * (1 - \frac{N:C}{(N:C)_{max}})\frac{\mathrm{NO}_s}{\mathrm{NO}_s + k_{\mathrm{NO}_s}}\frac{k_{in}}{k_{in} + \mathrm{NH}_s}CDZ$$
$$\mathrm{NH}_s{}^{\mathrm{uptake}} = \mathrm{NH}umax * f^T (1 - \frac{N:C}{(N:C)_{max}})\frac{\mathrm{NH}_s}{\mathrm{NH}_s + k_{\mathrm{NH}_s}}CDZ$$
$$\mathrm{PO_4}{}^{\mathrm{uptake}} = \mathrm{P}umax * f^T (1 - \frac{P:C}{(P:C)_{max}})\frac{\mathrm{P}}{\mathrm{P} + k_{\mathrm{P}}}CDZ$$
$$\mathrm{N_2}{}^{\mathrm{uptake}} = \frac{1}{2}(\frac{\mathrm{P}^{\mathrm{uptake}}}{PNRedfield_{diaz}} - (\mathrm{NH}_s{}^{\mathrm{uptake}} + \mathrm{NO}_s{}^{\mathrm{uptake}}))$$

D. Addition of dinitrogen

To complete the nitrogen cycle, the state variable representing dinitrogen (NTG) is also added to the model (2.2). Dissolved dinitrogen ($\mathrm{N_2}$) is produced by denitrification and anammox and removed by fixation.

$$\frac{\partial NTG}{\partial t} = \frac{\partial}{\partial z}(\tilde{\lambda}\frac{\partial NTG}{\partial z}) + \frac{1}{2}Denitrification + \frac{4}{3}ANAMMOX - \mathrm{N_2}{}^{\mathrm{uptake}}$$

The flux of dinitrogen across the air-sea interface is appended. According to the formulation of Wanninkhof ([62],[63]), this flux depends on a transfer coefficient (PistonVelocity) multiplied by the difference between a saturation concentration and the $\mathrm{N_2}$ concentration in sea water. The saturation concentration is estimated as the product of the gas solubility (solubility $\mathrm{N_2}$ (T,S) and the atmospheric pressure of $\mathrm{N_2}$ as explained in [63]. Coefficients for both Piston velocity solubility are taken from Wanninkhof ([63]). The calculation of solubility gives a dimensionless number (Bunsen coefficient) that is divided by the volume of one mole of N_2 under standard conditions of temperature and pressure, and multiplied by the partial pressure of dinitrogen in the atmosphere.

$$AirSeaNitrogenFlux = PistonVelocity * (\frac{0,78}{22.4148 * 0,000001}) * (SolubilityN_2 - SurfaceN_2)$$

All the equations and new parameters are in Appendix 4 and Appendix 4 respectively.

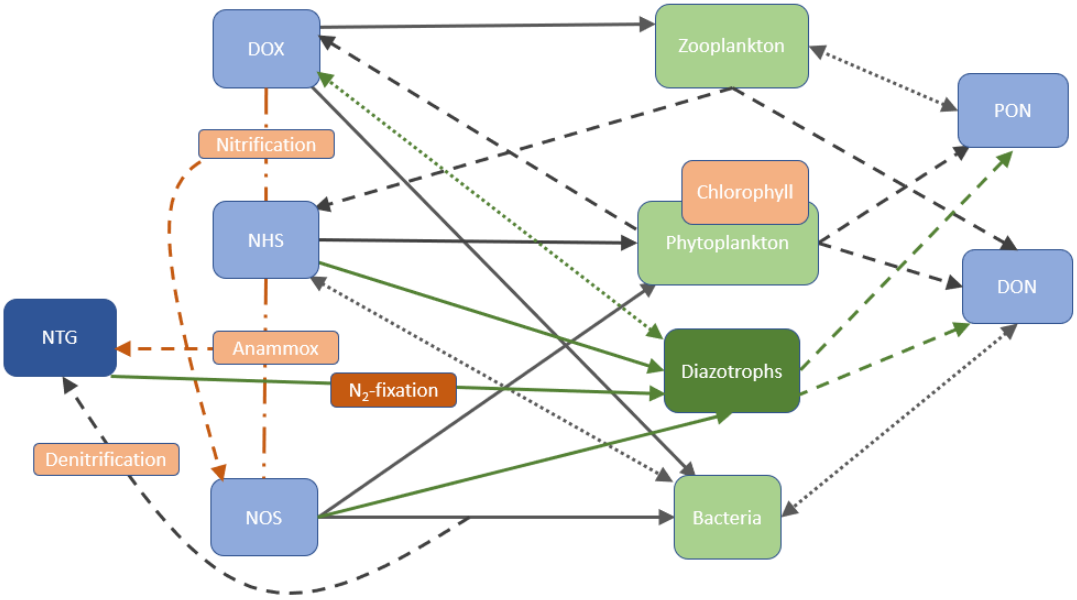

CHEMICAL STATE VARIABLES	DON	Dissolved organic nitrogen (encompasses labile and semi labile dissolved N)				
	PON	Particulate organic nitrogen				
	DOX	Dissolved oxygen				
	NHS	Ammonium + Ammonia				
	NOS	Nitrate + Nitrite				
	NTG	Dinitrogen				
BIOLOGICAL STATE VARIABLES	Bacteria	Bacteria				
	Zooplankton	Meso zooplankton + micro zooplankton + noctiluca + gelatinous				
	Phytoplankton	Diatoms + Flagellates + Emiliana				
	Diazotrophs	Diazotrophs				
CALCULATED OUTPUTS		Anammox	Denitrification	Nitrification	Chlorophyll	N_2-fixation
: biological reactions		: uptake by variable		: uptake and/or release		
: chemical reactions		: released/ variable		: combination of 2 molecules		
: new state variable		: new state variable				

Figure 2.2: **Schematic simplified representation of the nitrogen cycle in BAMHBI after addition of the new variables**

E. Additional diagnoses

The global budgets of each main component (i.e carbon, nitrogen, phosphate, silicate) are split into organic and inorganic budgets as well as a specific budget for fixed nitrogen. In addition, new diagnoses computing specifically the maximum and depth of maximum of oxygen, ammonium, nitrate and chlorophyll are estimated. Finally, the two conservative tracers suggested by Gruber ([23]) and Deutsch ([11]) are respectively computed as N^*= NOS - 16 PHO and P^* = PHO - NOS/16 as well as a $\frac{N}{P}$ratio. All of these extra diagnostics are shaped to allow a better understanding of the model dynamics.

2.1.3 The coupled model

The source code of BAMHBI is written in Fortran. However, the compilation, the links with NEMO and the outputs are performed in R. R is an open source project whose main pur-

pose is to provide a language and an environment for statistical analysis and graphs. Among the numerous available packages lie ”deSolve” and ”FME”. The first provides a performing tool to work on models using differential equations. Several integration methods are proposed. At the beginning, the integration routine was ”lsodar” that adapts the time step of integration. However, the use of explicit Euler integration method with a time step of 10 minutes showed a decrease in the number of non-convergent results while still preserving mass conservation. The second cited package derives from ”Flexible Environment for Mathematically Modelling the Environment - FEMME”, within which routines of sensitivity and calibration analyses are available. The description of those two packages can be found in [53](deSolve) and in [54] (FME).

The vertical grid of NEMO contains 31 levels that are interpolated to correspond to the 56 levels of BAMHBI. The first 100m comprises 15 boxes in NEMO and 32 in BAMHBI. In the latter, the thickness of the vertical meshes vary from 1m at the surface to 200m below the depth of 500 m. In both models, the thickness of the boxes increases with depth in order to solve the upper layer with an increased resolution.

The model has first been run over 2010 to 2016. However, some years (2013, 2015) stop running getting unusable. A reduction of coefficient diffusion solves this issue but does not seem to be justified. I decided then to run the model for 2016, repeating the forcing until steady-state.

A. Boundary conditions

Air-sea interface The atmospheric conditions (wind stress at 10m, cloud cover, precipitations) of the model are given by the European Center for Medium-Range Weather Forecasts (ECMWF) for the year 2016 at the same location as the NEMO 1D column (longitude of 35°37 E and latitude of 43°40 N). The zenith angle (zendeg) and the surface solar radiations (qsr) are needed in the calculation of the photosynthetic active radiation (PAR). The air-sea fluxes calculated in the model (O_2, DIC and N_2) are function of the mean wind speed at 10 m (wndm) ($wndm = \sqrt{{u_{10}}^2 + {v_{10}}^2}$.

Physical model Temperature, salinity, and the diffusion coefficient for 2016 are extracted from the 3D column NEMO and provided to force the 1D BAMHBI.

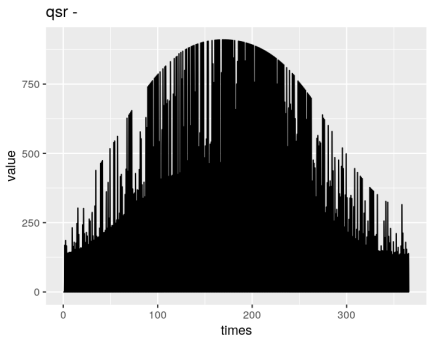

Figure 2.3: **Surface solar radiation (W/m^2), computed from astronomical formulation using the cloud cover from ECMWF**

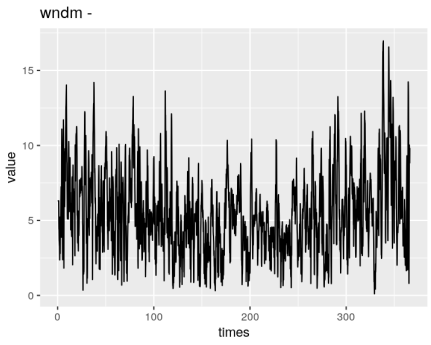

Figure 2.4: **Wind stress (m/s), from ECMWF**

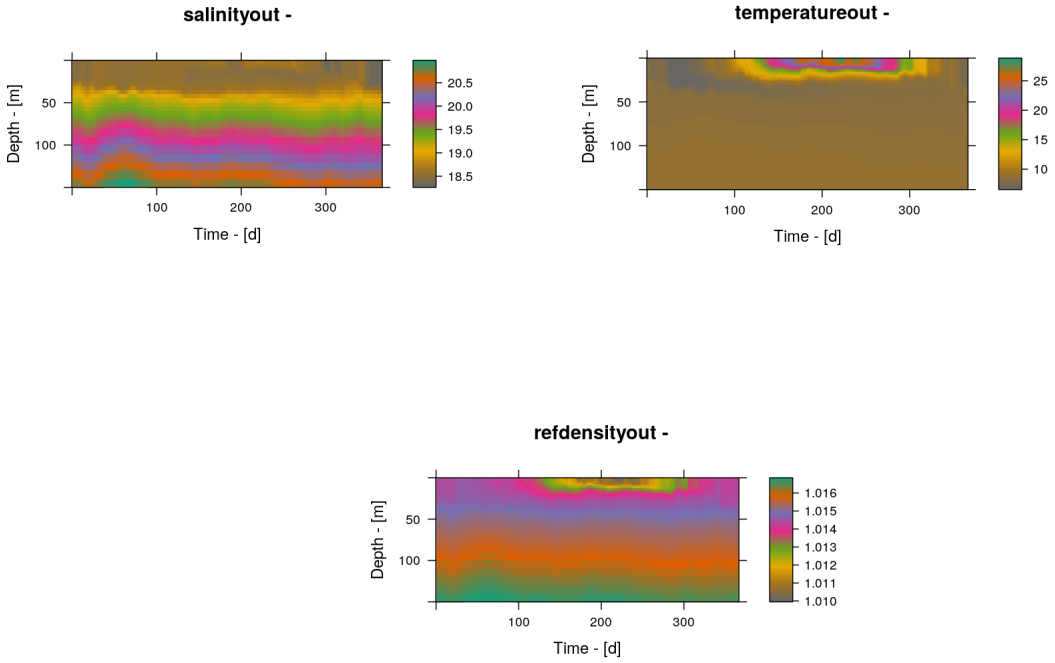

Figure 2.5: **Density (kg/m^3) vs depth**

An accurate representation of the vertical density structure is especially important in the Black Sea, as the concentration of the chemical compounds is strongly imprinted by the density vertical gradient. Also, it is well known that chemical properties exhibit peculiar features (gradient, maximum and minimum) that do not change in space or time when expressed on a density scale. Density (in kg/m^3) is calculated from in situ temperature and absolute salinity. The complete calculation is found in the R-package gsw documentation (https://cran.r-

project.org/web/packages/gsw/gsw.pdf).

B. Initial conditions

Biogeochemical model All of the biological state variables have the same vertical homogeneous profile. The inorganic compounds - inorganic nutrients (nitrate, ammonium, silicate, phosphate), dissolved gases (oxygen, dinitrogen) - have an interpolated profile from a WOD (World Ocean Database) dataset corresponding to the central basin of the Black Sea. The remaining variables (ODU, DIC, CHA) have also a typical profile of the same area converted from a density scale to a depth scale. I rebuild such initial grids.

C. Convergence to Steady State

The model has been run until reaching a steady state characterized by a repeated yearly cycle for all modelled variables. In order to obtain a constant nitrogen budget, a lateral transport in the form of NO_3, PO_4 and SiO_2 is imposed and computed at each time step. This transport is simulated by adding the computed losses of organic material into the corresponding inorganic variables :

- sunken organic carbon returns to DIC
- sunken organic nitrogen returns to NOS
- sunken organic silicate returns to SIO
- sunken organic phosphate returns to PHO

In addition, the losses of nitrogen due to denitrification, anammox, and oxidation of ODU by nitrate are redistributed into NOS.

Both the depth at which the material is removed from the water column (parameter k-redistribute) and the total depth over which the material is redistributed need to be parametrized (parameter redistribute-bottom-flux-top). A balanced solution is found when the sunken material is taken at 150m and redistributed over the first 100m of the water column (see section 2.2.B).

D. Sensitivity analyses

A sensitivity analysis is performed once the parameters have been tuned by hand. Such an exercise can explain how changes in the parameters estimates may impact the output of the model. It can therefore be used to test the robustness of the model or to explain the consequences of uncertainty in parameter values. Both global and local sensitivity analyses are considered. The package FME, in R, provides the necessary tools to carry out the two types of sensitivity tests (function sensRange and sensFun respectively)([54]).

Global sensitivity All of selected parameters are modified within a chosen range. The effect of such a variation is estimated on chosen output variables. The selection of a set of parameters gives information about the global sensitivity of the model regarding these parameters while the analysis of one single parameter can help establish cause and effect relationships.

Local sensitivity This test focuses on the quantitative effect of an infinitesimally small change in one parameter value on the model output. When "sensFun" is called, it creates a matrix in which the calculated sensitivity of chosen parameters on certain variables is stored. The element (i,j) of the matrix is the result of

$$\frac{\partial y_i}{\partial \theta_j}\frac{w_{\theta_j}}{w_{y_i}}$$

y_i is the output modelled variable, with the scaling w_{y_i} (equal to its initial value) and θ_j is the tested parameter, with the scaling w_{θ_j}(equal to its value). The summary returns a data frame containing the minimum, maximum and mean values of the sensitivity function, as well as the L1 norm and the L2 norm which are defined as follow :

$$L1norm : \frac{\Sigma|(S_{ij})|}{n}$$

and

$$L2norm = \sqrt{\frac{\Sigma(S_{ij})^2}{n}}$$

Values of L1-norm and L2-norm allow a ranking of the parameters from the more to the less influential on the model and a selection of the most sensible parameters can be decided for further analysis/calibration.

However, depending on the number of parameters to analyze, it can also be useful to search for interaction between parameters. Additional tests can be performed following the local sensitivity analysis. First, the correlation between two parameters can be evaluated by the function

"pairs". This function returns plots of the relationship between two parameters and adds the r^2 of the set. It allows to find identifiable pairs of parameters. However, some models possess a large number of variables and identifiability may be challenging. In this case, a second type of identifiable analyses, collinearity, can be undertaken. This differs from the previous one by allowing an estimation of the approximate linear dependence between more than two parameters. The collinearity index (γ) is computed from the sensitivity matrix.

$$\gamma = \frac{1}{\sqrt{min(EV[\hat{S}^T \hat{S})}}$$

where $\hat{S}_{ij} = \frac{S_{ij}}{\sqrt{\Sigma_j S_{ij}^2}}$. $\hat{S}$ contains the columns of the sensitivity matrix corresponding to the selected parameters, EV estimates the eigenvalues ([54]). A high collinearity index between two parameters means that a change in one of them can be compensated by a change of the other.

CHAPTER 3

RESULTS AND DISCUSSION

3.1 Model without diazotrophs

The model is run for 20 years to reach a steady state and the 21^{st} year is presented. The analysis of the graph of chlorophyll shows presence of chlorophyll between 50-70m during the year, with a maximum of 0,8 mg Chl m^{-3} in autumn. Two peaks of chlorophyll are observed at different depth, the deepest being the most important.

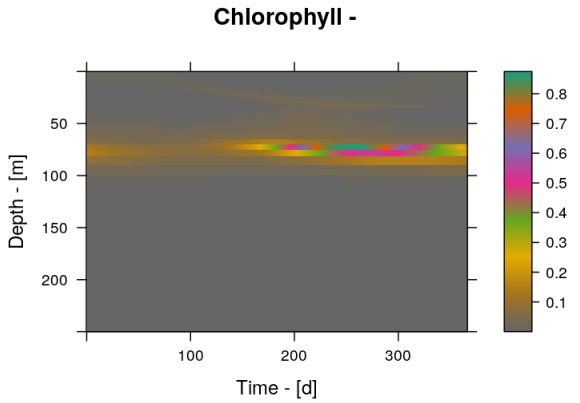

Figure 3.1: **Chlorophyll (mg Chl m^{-3})**

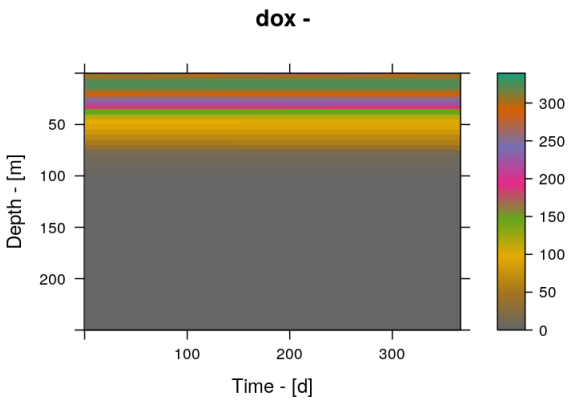

Figure 3.2: **Oxygen (mmol O_2 m^{-3})**

The maximum of oxygen is observed at the subsurface. The oxycline lies around 50 m while there is no more oxygen below 100m. The maximum concentration of nitrate (7 mmol N/m^{-3}) is observed at a constant depth of 80m which is typical of the nitracline. Its production by

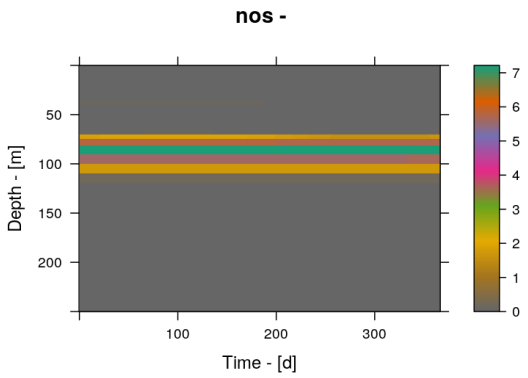

Figure 3.3: **Nitrate (mmol N/m^{-3})**

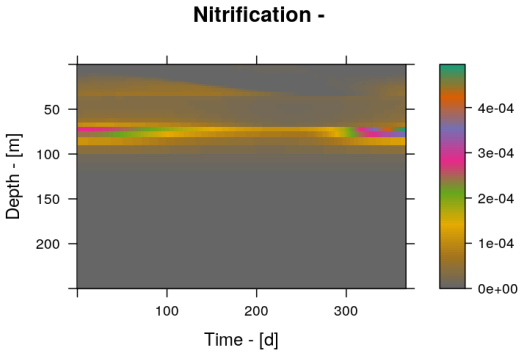

Figure 3.4: **Nitrification (mmol N/m^{-3} d^{-1})**

nitrification happens in the first 100m of the water column, mainly between 70 and 100m where organic matter is degraded. Nitrate is then consumed by anammox reaction. Anammox reaction and denitrification take place at the same depth, between 70 and 120m. They both occur once the oxygen concentration is very low. Even though the reaction is observed all the year long, the maximum rate of anammox (0,00020 mmol N m^{-3} d^{-1}) happens in winter, once the organic matter has sunken after the phytoplanktonic bloom. Denitrification rates are a hundred times smaller than those of anammox reaction.

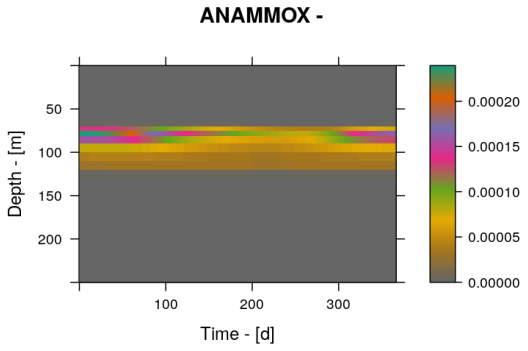

Figure 3.5: **Anammox (mmol N m^{-3} d^{-1})**

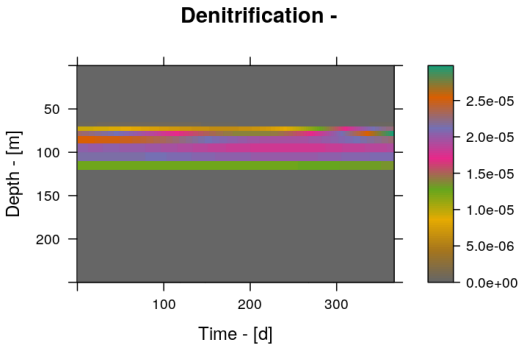

Figure 3.6: **Denitrification (mmol N m^{-3} d^{-1})**

Additional graphs are in Appendix 4

3.2 Model with a complete nitrogen cycle

Chlorophyll and phytoplankton

To begin with, the chlorophyll concentration (fig. 3.7) is within the expected range for the Black Sea ([48], [9]). Chlorophyll can be observed all year long from the surface to 70-80m deep and two peaks of chlorophyll are observed at different depth. A subsurface peak of chlorophyll lies between 0 and 30m (0,1 to 0,4 mg Chl m^{-3}) while the second one is located at a depth between 40 and 70m and is more important (up to 1 mg Chl/m^3).

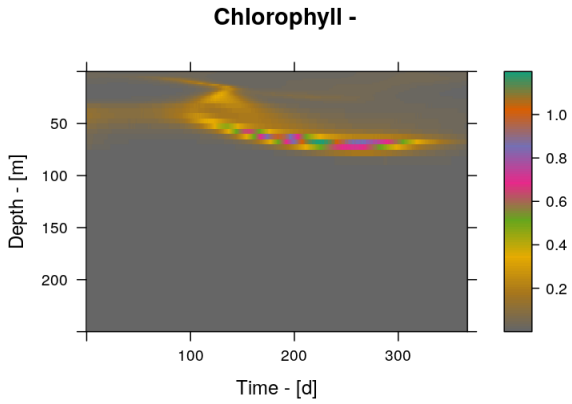

These patterns are consistent with what was seen before addition of the new functional group (fig. 3.1). However, the modelled deep chlorophyll maximum (DCM) is always too deep for the Black Sea (around 70m) while BGC-Argo derived DCM is rarely below 50m ([48], [8]).

Figure 3.7: **Chlorophyll (mg Chl m^{-3})**

The different blooms of the different phytoplankton groups are well detected on the graph of the chlorophyll content. The two main groups are diatoms (fig. 3.8) and diazotrophs (fig. 3.9). Both groups are present all year long but their distribution differs. There is a first bloom of diatoms in spring at a depth of 30-50m and a second, deeper ($\sim$ 70m), in summer. At the end of autumn, diatoms are approximately 70m deep. During the first bloom their maximum concentration reaches 1,5 mmol C m^{-3} although the peak is at 2 mmol C m^{-3} during summer.

As for diazotrophs, they are present all year long at low concentration and at a depth of 30 to 50m. A slightly deeper bloom (60-70m) occurs in late summer and fall during which their concentration reaches 3,5 mmol C m^{-3}. The maximum of chlorophyll corresponds to the superposition of the summer bloom of each species.

The last two phytoplanktonic groups (Emiliana (fig. 3.10) and Flagellates (fig. 3.11)) account for less total chlorophyll content. The two species are present at low concentration all year long as well. An early spring bloom of Emiliana is observed (maximum concentration 0,8 mmol C m^{-3}) in the first 30m of the water column. Flagellates are the smallest group of all

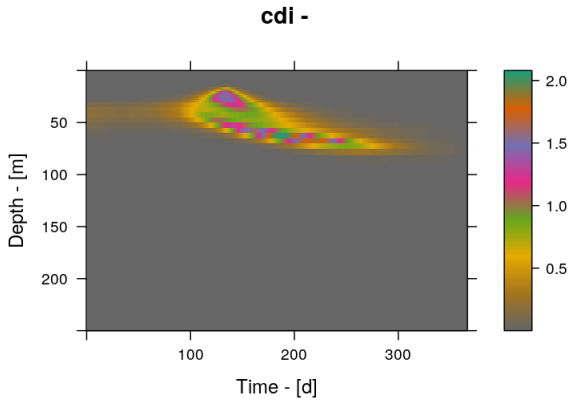

Figure 3.8: **Diatoms** **(mmol C m^{-3})**

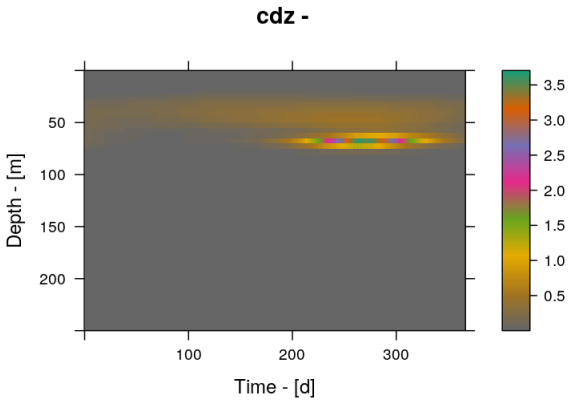

Figure 3.9: **Diazotrophs** **(mmol C m^{-3})**

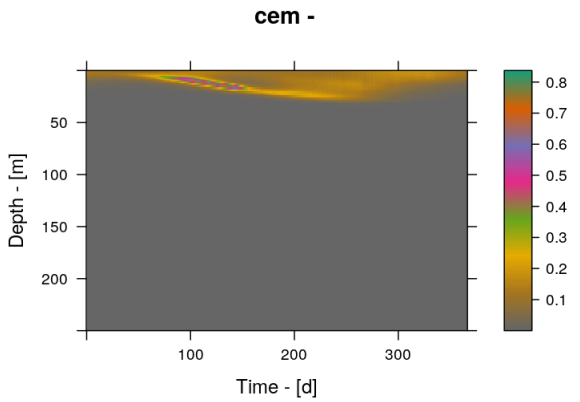

Figure 3.10: **Emiliana** **(mmol C m^{-3})**

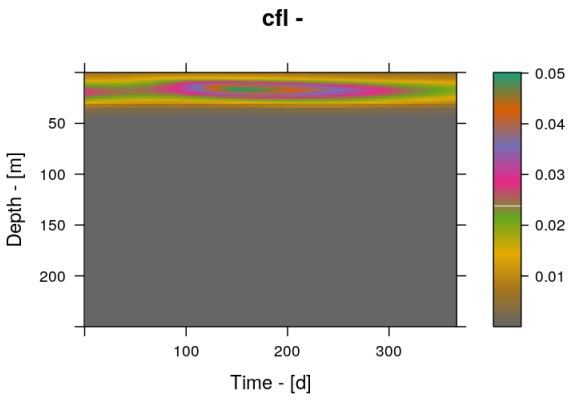

Figure 3.11: **Flagellates** **(mmol C m^{-3})**

and live up to 40m depth. Their maximum concentration hardly reaches 0,05 mmol C m^{-3} in spring.

Diazotrophs

As mentioned in the previous section, the bloom of diazotrophs happens in late summer and fall at 60-70m depth. When presented in nitrogen content instead of carbon, their maximal concentration is about 0,6 mmol N m^{-3} (fig. 3.12). Based on the physiology of the well-studied *Trichodesmium*, diazotrophs are modelled as facultative fixers. They can thrive in the water without fixing dinitrogen but have the ability to switch to N_2 fixation if necessary (like what was made by Paulsen et al., [47] or [44]). This is well represented in the model (fig. 3.12, 3.13 and 3.14). The growth of diazotrophs does not rely on N_2 fixation alone and uptake of N_2 is only observed when fixed N is limiting (mainly during the autumnal bloom but also after the

spring bloom).

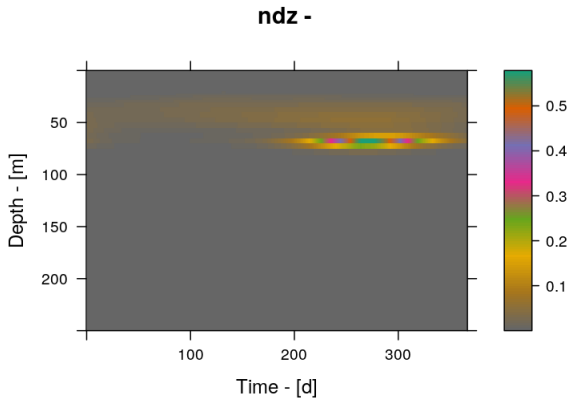

Figure 3.12: **Diazotrophs (mmol N m^{-3})**

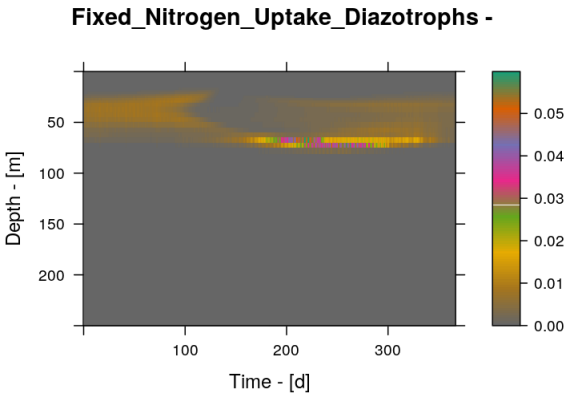

Figure 3.13: **Uptake of fixed N by diazotrophs (mmol N m^{-3} d^{-1})**

The model simulates that most of the time diazotrophs use fixed nitrogen to grow (fig. 3.13). N_2 fixation is mainly observed during the fall peak of cyanobacteria (fig. 3.14) but an additional period of N_2 fixation is present during spring, at shallower depth.

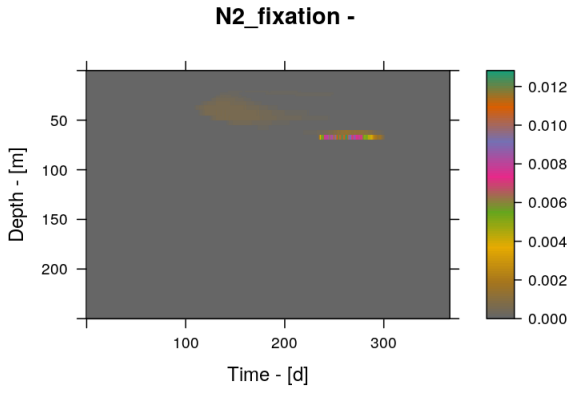

Figure 3.14: **N_2 fixation (mmol N m^{-3} d^{-1})**

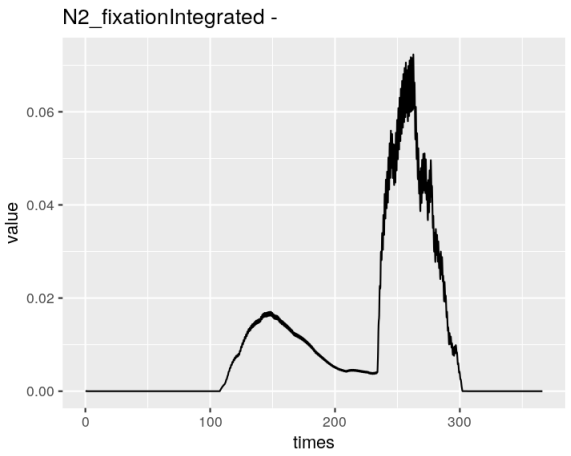

Figure 3.15: **Integrated N_2 fixation (mmol N m^{-2} d^{-1})**

It is worth noting that N_2 fixation is continuous from April to October (day 100 to day 300) (fig. 3.15). Even if the uptake rate of N_2 is as little as 0,005 mmol N $m^{-2}d^{-1}$ between the two periods of higher fixation, it remains present. The maximum rate of N_2 fixation is a little bit higher than 0,007 (mmol N $m^{-2}d^{-1}$) in late summer, while values between 0,01 and 0,02 mmol N $m^{-2}d^{-1}$ are observed in spring. This can be explained by the consumption of fixed N during

other phytoplankton groups bloom, depleting the waters in fixed nitrogen and thus triggering the fixation of dinitrogen.

It is highly difficult to evaluate the relevance of such a result, because N_2 fixation in the Black Sea is not well known. The depth at which N_2 fixation is performed in the Black Sea is also difficult to apprehend. In the basin, chemobacteria able to fix N_2 have been identified in the suboxic waters as well as in the upper part of the sulfidic layer by Pshenin in the 1970's - 80's ([41]) and Kirpatrick ([30]) thirty years later. Rates of N_2 fixation have also been measured by McCarthy ([41]) in both the euphotic and aphotic zones in 1999 and 2001. In the euphotic zone, McCarthy recorded N_2 fixation only at two stations, at maximum values of 75 nmol N $kg^{-1}d^{-1}$, while Fuchsman calculated N_2 fixation rates twice as large and Sorokin in 2002 found a rate of about 20-40 nmol N $kg^{-1}d^{-1}$ (given by [66])(see paragraph 1.3.2). All of these results are higher than ours (maximal values of about 12 nmolN $kg^{-1}d^{-1}$, fig. 3.14). This, of course, can be explained by shortcomings in the model, as it is a first attempt.

To predict whether diazotrophic organisms could grow, the conservative tracer suggested by Gruber ([23]) is created : N^*= NOS - 16 PHO (see paragraph 1.3.1). Places where N^* is negative are areas where a net sink of fixed N is observed and therefore may be thought as places where N_2 fixers could be favoured by their capacity to fix N_2. Indeed, N_2 fixers will consume proportionally more phosphorus than non-diazotrophic phytoplankton. N^* should therefore remain constant where non-diazotrophic phytoplankton thrive.

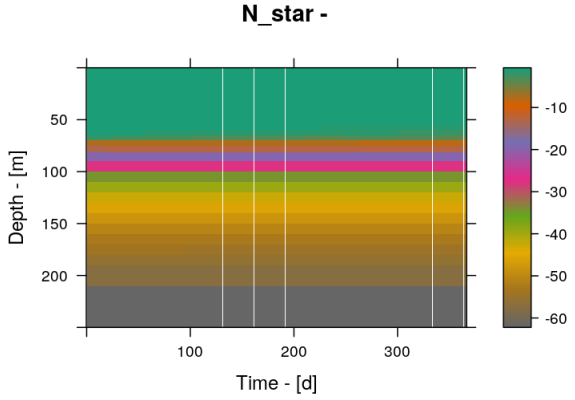

Figure 3.16: **N^***

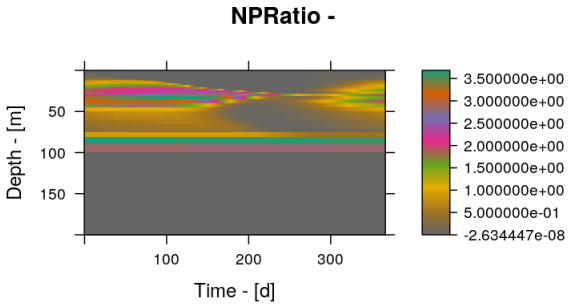

Figure 3.17: **N:P ratio**

Results show that N^* (Fig.3.16) is negative but close to 0 up to 60-70m. One of the reasons may be because the formulation is a little simplified compared to what Gruber proposed. However, even if a correcting term were added, the value of N^* would probably become rapidly

negative as the basin is known to be a sink of fixed nitrogen ($\sim$ 9 10^{10} mmol N yr^{-1} for the basin according to Grégoire ([19]). Slight differences in N^* that would show N_2 fixation cannot be spotted at this graph scale. Nevertheless, the figure of the N:P ratio (fig. 3.17) has values lower than 4 that is typical of the upper layer of the Black Sea and suggests the presence of N_2 fixers ([15]).

Nitrogen cycle and oxygen

The two main sources of nitrogen for diazotrophs are N_2 and nitrate. Dinitrogen (max 560 mmol N_2 m^{-3}, fig.3.18) and nitrate (max 7 mmol N m^{-3}, fig.3.19) concentrations are maximal close to their production depth (respectively between 100m and 120m for the former and 80 m for the latter). In the water, denitrification and anammox increase N_2 concentration, while the only way to remove it is through dinitrogen fixation. Nitrate decreases due to its consumption by phytoplankton as well as denitrification and oxidation of ammonium and ODU[1]. It is produced by nitrification.

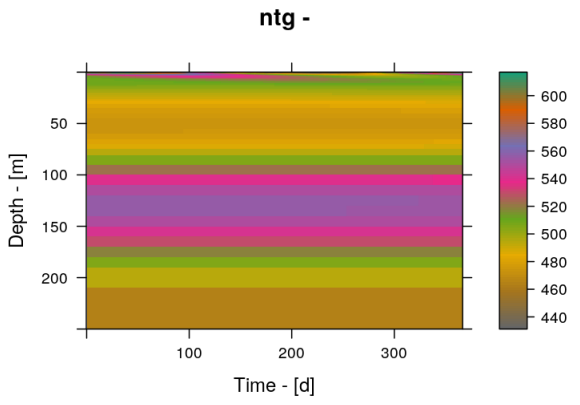

Figure 3.18: $\mathbf{N_2}$ **(mmol N** $\mathbf{m^{-3}}$**)**

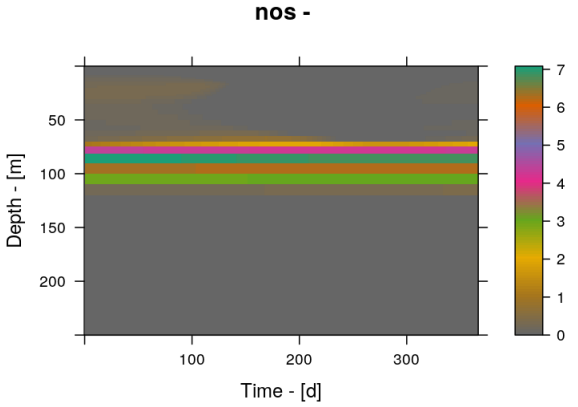

Figure 3.19: **Nitrate (mmol N** $\mathbf{m^{-3}}$**)**

[1]ODU = Oxygen demand unit, encompasses all the reduced molecules not explicitly modelled

At the surface, the N_2 concentration varies following the air-sea flux (fig. 3.20). An upward flux means N_2 enters the water, which happens in winter.

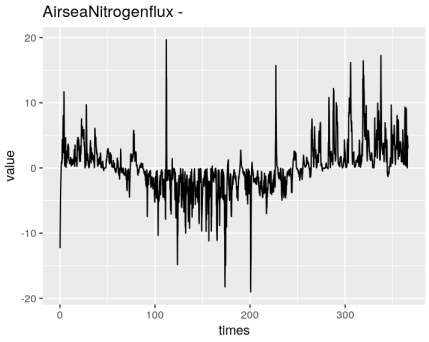

Figure 3.20: **Air-sea flux of N_2 (mmol N m^{-2} s^{-1})**

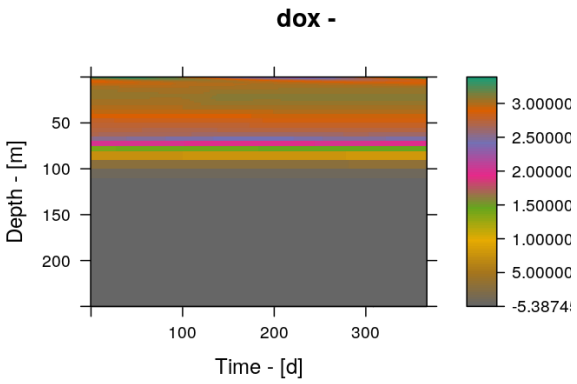

Figure 3.21: **O_2 (mmol O_2 m^{-3})**

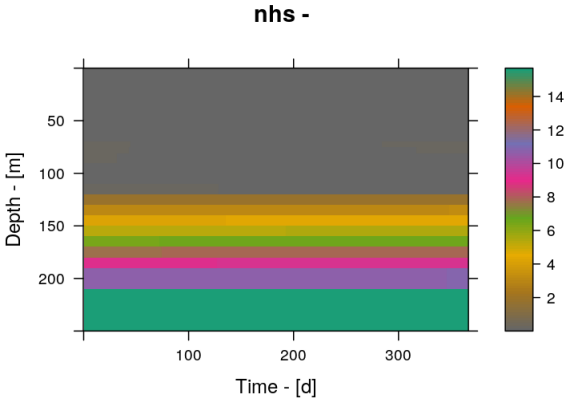

Figure 3.22: **Ammonium (mmol N m^{-3})**

Oxygen (fig.3.21) is produced in the uppermost layer by primary production, while it is removed from the water column by planktonic and oxidation of NHS and ODU. Oxygen concentration is maximum at the subsurface (above 300 μM). The oxycline is observed between 80 and 100m, and oxygen disappears below 110m. The depth at which O_2 reaches concentrations lower than $10\mu M$ influences both the depth of anammox reaction and denitrification, as they are inhibited by the presence of oxygen.

Ammonium (fig.3.22) is consumed by phytoplankton and bacteria when available, and removed from the water column by nitrification and anammox reaction. Ammonium concentration is close to zero in the first 120m of the water column, even if some sporadic spots of higher concentration can be observed. These are linked to the excretion of ammonium by both phytoplankton and zooplankton but this ammonium is immediately oxidized into nitrate. Below 120m, in absence of O_2 its concentration rapidly increases from 2 to 15 mmol N m^{-3} at 250m.

Vertically integrated rates of denitrification (fig.3.23) and anammox (fig.3.24) reaction show a similar profile throughout the year. The maximum values are observed at the beginning of the year immediately followed by a decrease until mid-year. The minimum rate value is found during the summer. Even though the minimum rate of denitrification is reached earlier than the one of anammox reaction, the two processes exhibit an increasing rate during the fall. A second maximum is observed in winter.

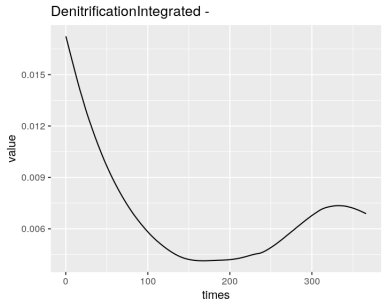

Figure 3.23: **Denitrification Integrated (mmol N $m^{-2}\mathbf{d}^{-1}$)**

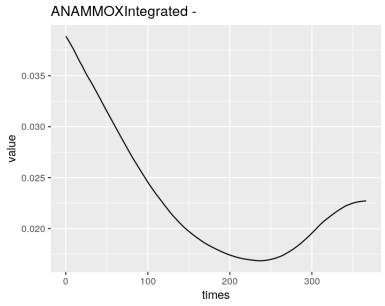

Figure 3.24: **Anammox Integrated (mmol N $m^{-2}\mathbf{d}^{-1}$)**

Anammox rates vary between $\sim$ 0,017 and $\sim$ 0,038 mmol N $m^{-2}d^{-1}$ while denitrification rate is smaller (0,004 mmol N $m^{-2}d^{-1}$ - 0,017 mmol N $m^{-2}d^{-1}$). The pattern of the two processes is shaped by the dynamic of the bloom with the maximum of chlorophyll attained in late summer and fall. The decomposition of the organic matter makes molecules (i.e NO_3, NH_4) available for these processes to happen while winter mixing seems to enhance anammox.

A close link between denitrification and N_2 fixation has been shown by Deutsch ([11]) while δ^{15}N analyses made by Fuchsman and by Konovalov also show that there is a close link between denitrification, anammox reaction and N_2 fixation in the Black Sea (paragraph 1.3.2). This may not be the case in the global ocean, as suggested by Wang ([60]) this year. They noticed the decoupling between denitrification and N_2 fixation, placing the former in the upwelling zones of the eastern tropical Pacific and Arabian Sea subtropical gyres and the latter in the subtropical gyres. They hypothesized that a lack of iron could prevent diazotrophs to thrive in waters otherwise impoverished only in NO_3^-. Their model did not represent varying seasons. In addition, they considered only cyanobacteria as diazotrophs. Yet, heterotrophic bacteria able to fix N_2 are numerous and taking them into account could lead to different results. Fernandez ([14]) provided evidence of high rates of N_2 fixation in the Eastern Tropical South Pacific (ETSP) in 2005 and 2007, measured at a depth from the surface to 400m. The maximum rates were obtained in the low oxygenated layer. The genetic analyses of sampled waters revealed

the presence of various genes *nifH* (a necessary gene to perform N_2 fixation) suggesting that different plankton could perform the fixation. Few of those genetic sequences matched those associated to cyanobacteria. All those researches prove how difficult it is to correctly represent the place of N_2 fixation in the global nitrogen cycle. In this model, only one sort of diazotroph is represented (cyanobacteria) but still they found a niche in the water column. On the graphs, they turn to N_2 fixation (figures 3.14) just above a slight spot where denitrification is present (fig.3.25). This is to take cautiously, as denitrification should not happen in this place (too high

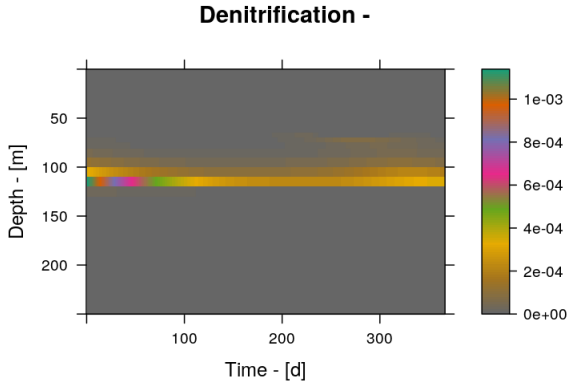

Figure 3.25: **Denitrification (mmol N m^{-3} d^{-1})**

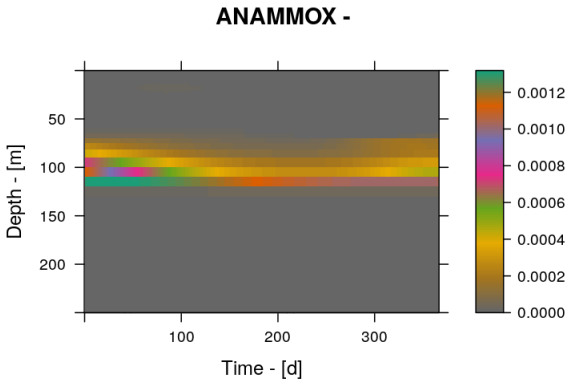

Figure 3.26: **Anammox (mmol N m^{-3} d^{-1})**

levels of oxygen). However, the appearance of denitrification at the same time as N_2 fixation is intriguing and will need further investigations. Denitrification is maximal at a depth of 120 m, which is within the suboxic layer as described by Konovalov ([33]) ($\sigma_t \approx$ 15.6 and 16.2) and Yakushev ([67]) (see graph 2.5). The rate of denitrification ($\sim$0.0017mmol N $m^{-3}d^{-1}$) is in agreement with the rate modelled by Yakushev ([66]) while Ward and Kirlpatrick (1991) had measured 0.002 μM N d^-1 ([66]). Nonetheless, denitrification can be absent in the water column ([26]). According to Jensen ([26]), the anammox process is not completely inhibited by oxygen but can happen at concentration of O_2 up to 13 μM. This reaction can therefore take place in a thicker layer than for denitrification. The model reproduces this difference between the two reactions, as anammox extends from 75 to 120 m (even though and as for denitrification, the reaction should have not happen at that high levels of oxygen). The rate of anammox ($\sim$ 0,0013 μM N d^{-1}) is in the range of the rate modelled by Yakushev ([66]) (0–0,03 μM N d^{-1}), with a little higher maximum value.

This superposition of denitrification/anammox reaction and oxygen is not apparent as long as

the model is run without the diazotrophs (see fig.3.2, 3.5, and 3.6). The oxycline deepens once N_2 fixers are added while the highest layer in which denitrification happens rejoins the oxic layer. The probable reason is that diazotrophs were voluntary tuned to have little light limitation in order to cover the maximum possible of the euphotic zone and identify potential niches. The equations are based on those of the phytoplankton as diazotrophs are modelled as cyanobacteria. Therefore, they release oxygen. As they are mostly confined in the deepest part of the euphotic zone, they add oxygen in the water at an unusual depth for the basin. As a result, the thickness of the layers of denitrification and anammox reaction are reduced compared to the model without N_2 fixers. The choice of adding diazotrophs as a group of cyanobacteria was driven primarily by the fact this group is best known and represented in several models ([45], [44], [47], [35]), Kuhn ([35]) being the only one to have represented both autotrophic and heterotrophic diazotrophs (in the Red Sea). Several tests are considered to prevent the oxycline to deepen. Physiologically, higher respiration rates have been observed in *Trichodesmium sp.* when they fix N_2 ([45]). This additional consumption of O_2 during periods of N_2 fixation contributes only a little to the total respiration ([44]) and is already taken into account in the model. Model results show little sensitivity to the parameter DFixDiaz[2] (L1norm = 0,000025 on integrated $[O_2]$). However, a sensitivity test on the oxygen threshold in the suboxic layer has not been modeled and should probably have given different results. When this parameter is increased, the oxygen concentration at depth improves and denitrification and anammox reaction do not coincide anymore with the base of the oxycline. A sharp increase of respiration gives the best results.

The oxycline (fig.3.28) is much better represented than in the previous simulation and dinitrogen fixers (fig.3.27) are found slightly deeper (75-80m). In this simulation, the two peaks of chlorophyll are present but the chlorophyll content results mainly from the diazotrophs, so the DCM is at about 75-80m as well (fig.3.29). The maximum N_2 fixation rate (fig.3.30) is higher in this simulation than in the previous one (respectively 0,020 mmol N m^{-3} d^{-1} and 0,012 mmol N m^{-3} d^{-1}) and then is more realistic in terms of intensity and spatial distribution. Unlike the precedent simulation, the reaction is observed at only one depth ($\sim 75m$) and lasts longer.

The maxima of denitrification (fig.3.32) and anammox (fig.3.31) in the water column are comparable to the previous simulation (slightly higher) and are still within the expected ranges. However, the vertically integrated rates of the two reactions are smaller.

[2]related to the additional respiration of diazotrophs due to N_2 fixation

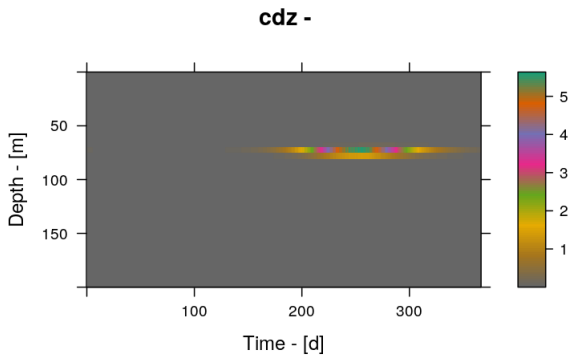

Figure 3.27: **Diazotrophs** (mmol C/m^3)

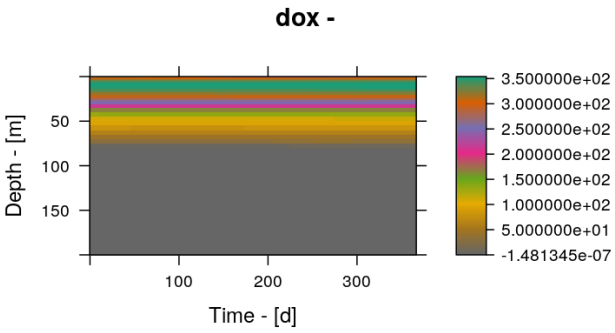

Figure 3.28: **Oxygen** (mmol O_2/m^3)

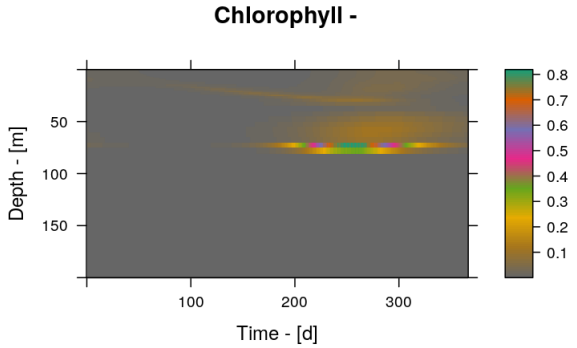

Figure 3.29: **Chlorophyll** (mg Chl/m^3)

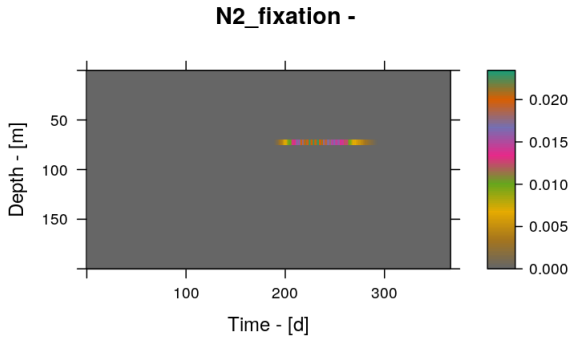

Figure 3.30: N_2 **fixation** (mmol N/$m^3$$d^{-1}$)

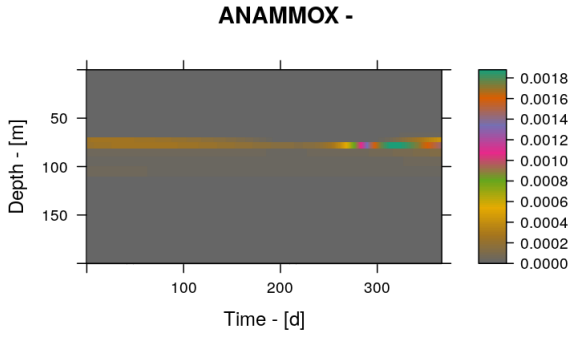

Figure 3.31: **Anammox** (mmol N/$m^3$$d^{-1}$)

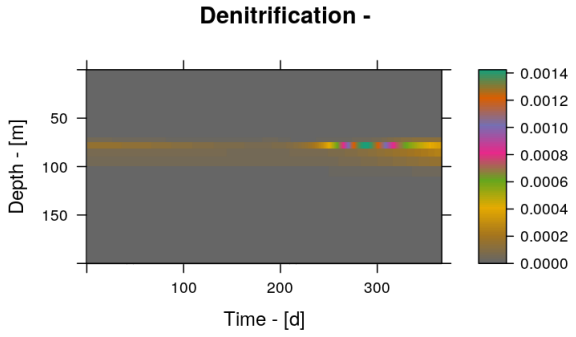

Figure 3.32: **Denitrification** (mmol N/$m^3$$d^{-1}$)

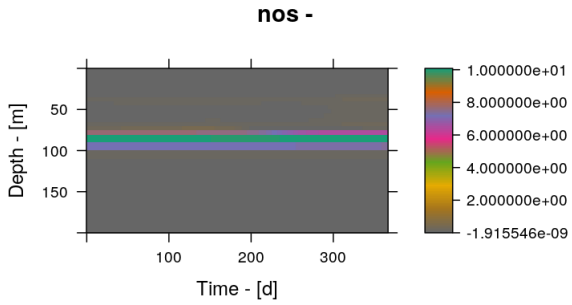

As observed previously, these maxima immediately follow the bloom of diazotrophs, practically at the same depth.

The concentration of nitrate is too high, even though it lays at a correct depth.

Figure 3.33: **Nitrate (mmol N/m^3)**

The sharp increase of respiration is purely empirical and does not rely on the literature. The only purpose doing so is to avoid anomalies in the oxygen content and in the highest depths at which denitrification and anammox reaction happen. Nonetheless, it provides useful information regarding diazotrophs. First, they seem to thrive at the lowest possible depth. They seem somehow related to anammox reaction and denitrification. However, this excessive production of O_2 might not be completely unrealistic as the oxidation of sulfide diffusing from the euxinic layer is still enigmatic. Indeed, Konovalov ([34]) find that diffusion of O_2 computed from the typical O_2 profile is not high enough to oxidize this sulfide but rather the lateral transport of O_2 from the Bosporus could be the mechanism by which O_2 is brought to the suboxic layer.

Budgets

As most of the processes happens above 150m, the nitrogen budget and the fixed nitrogen budget are integrated over this depth. The upper nitrogen budget is the sum of all nitrogen species, both organic and inorganic. The upper fixed nitrogen budget comprises only nitrate and ammonium. It should be noticed that the scale of the two graphs are highly different, as the mean upper N budget is roughly 250 times higher than that of fixed nitrogen. The latter is therefore much more impacted than the former by any change in the budget.

The general trend is similar for both budgets. The sharp diminution is in linked to the consumption by plankton during the spring and summer. The remineralization process begins mid-summer. The decrease observed on the upper fixed budget begins a little earlier and shows a deceleration at the beginning of the summer. These observations can not be made on the first graph, because it includes other nitrogen species and then a difference in the scaling.

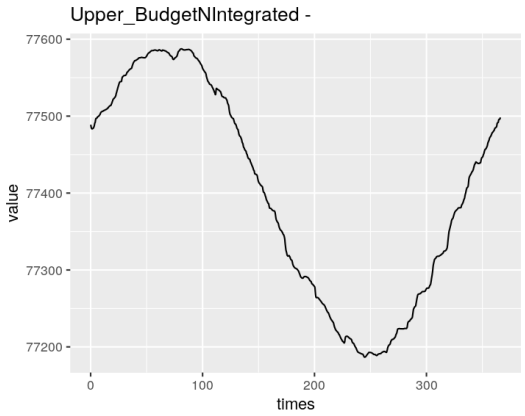

Figure 3.34: **Total N budget**

(vertically integrated over 150m, mmol N m^{-2})

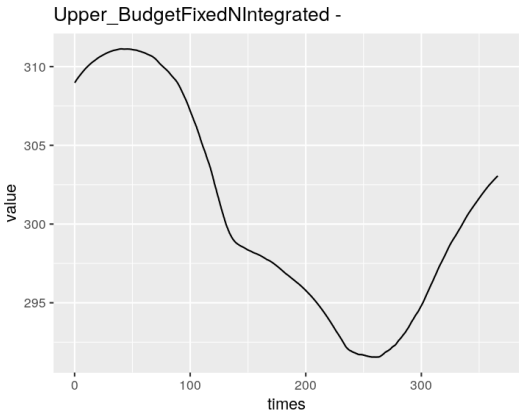

Figure 3.35: **Total N budget**

(vertically integrated over 150m, mmol N m^{-2})

3.3 Sensitivity

The sensitivity of model results to the 20 parameters describing the dynamics of diazotrophs (referred as NFP) as well as to the 10 parameters involved in anammox and denitrification (referred as CP) is assessed using the FME package. The variables and diagnostics are all integrated over the first 150 m of the water column. We proceed as follows. First, global and local sensitivity analyses are performed perturbing the parameters associated to respectively diazotrophs and denitrification/anammox modelling. Based on the impact on selected modelled variables, those parameters are ranked and we limit the presentation of the analyses to the most sensitive ones.

Except for the maximum uptake of ammonium by diazotrophs, all parameters linked to the nitrogen uptake (e.g. maximum uptake rate, half-saturation constant) show little impact on the local sensitivity test. This is explained by the fact that diazotrophs are never limited in nitrogen. A low sensitivity is also observed for parameters of additional respiration (DFix Diaz) and attenuation coefficient (bbdzt short and long). Furthermore, some diagnoses are very insensitive to all tested parameters (maximal NOS, NHS and DOX - quantity and depth).

All of the chemical parameters showed little local sensitivity.

Table3.1 summarizes the L1-norm ($L1norm : \frac{\Sigma|(S_{ij})|}{n}$) of the most sensitive parameters regarding nitrogen fixers (NFP) for selected diagnoses. The complete list of tested parameters and diagnoses is referenced in Appendix 1. The description of the parameters is found in Appendix 4.

Interestingly, the internal minimal and maximal N:C ratios show the biggest sensitivity on

	1	2	3	4	5	6
MinNCrDiazotrophs1	9,1	10	11	2,5	4,5	24
MaxNCrDiazotrophs1	8,5	9,7	11	2,3	4	40
MortalityDiazotrophs1	5,1	5,6	6,1	1,3	2,4	16
alphaPIDiazotrophs1	5	5,6	6	1,4	2,5	12
Q10Diaz1	3,7	4	3,9	0,9	1,6	8
MuMaxDiazotrophs1	2,3	2,5	2,7	0,62	1,1	5,4
PNRedfieldDiaz1	1,1	1,3	0,94	0,48	0,6	6,3
PO4MaxUptakeDiazotrophs1	0,92	1	0,9	0,24	0,39	6,4
ksPO4Diazotrophs1	0,68	0,73	0,69	0,17	0,28	4,8
NHsMaxUptakeDiazotrophs1	0,002	0,0032	0,29	0,015	0,0034	1,8

Table 3.1: **L1 norm for selected parameters**
Each column represents the impact on selected modeled variables, all of them being vertically integrated : 1. Biomass diazotrophs in carbon, 2. Chlorophyll from diazotrophs, 3. Fixed nitrogen uptake by diazotrophs, 4. Anammox, 5. Denitrification, 6. N_2 fixation

the widest range of outputs. Not only do they impact the biomass of diazotrophs, their uptakes in N_2 and in fixed nitrogen and the subsequent chlorophyll (those were expected), but also denitrification and anammox reaction. With the higher L1-norm for all parameters, the N_2 fixation diagnostic is the most sensitive of all. The results of the last column need to be taken carefully as some of them are systematically likely outliers. However, the global sensitivity test performed on dinitrogen fixation is highly reactive (fig.3.40).

Biomass of diazotrophs

The total biomass of diazotrophs shows large variations when a global sensitivity with parameters regarding their growth is performed. In addition, it seems that the peak of N_2 fixers could happen earlier than what is obtained by the model. The biggest sensitive parameter for the biomass is the $(N:C)_{min}$ ratio. When taken alone and within a range of 0,8-1,2 from its initial value, it already shows a large variability (see fig.3.37).

The graph of the local sensitivity test confirms that the two most sensitive parameters regarding vertically integrated biomass are $(N:C)_{min}$ and $(N:C)_{max}$ ratios. In addition, it shows that the effect of the two parameters on the model result are opposed to each other. This rela-

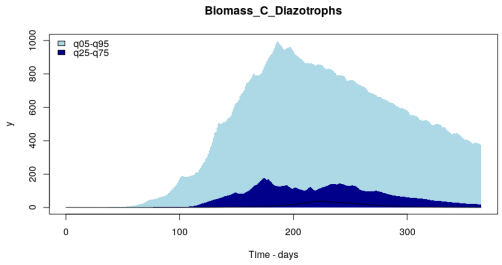

Figure 3.36: **Global sensitivity on the biomass of diazotrophs to NFP**

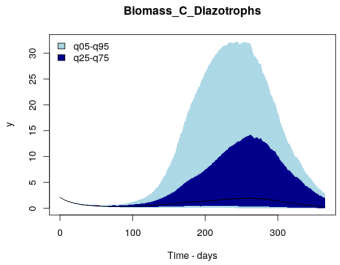

Figure 3.37: **Global sensitivity on the biomass - NCr min (0,8-1,2)**

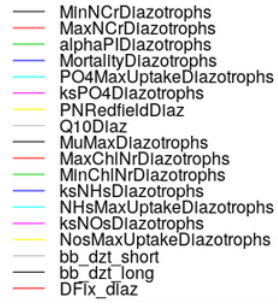

Figure 3.38: **Legend for local sensitivity graphs**

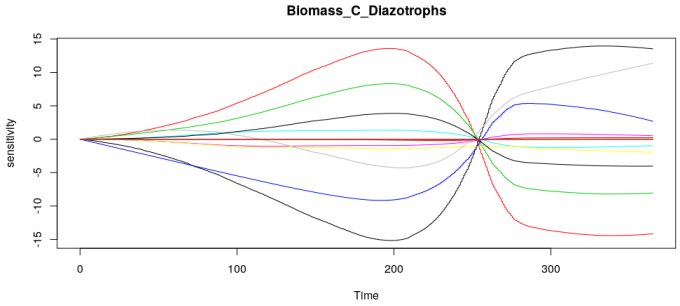

Figure 3.39: **Local sensitivity of NFP on the biomass**

tionship is also noticed for the next two more sensitive parameters (mortality rate and αPI[3]). An inversion of the effect of all parameters on the model happens at the same time, at the end of the bloom.

N_2 fixation

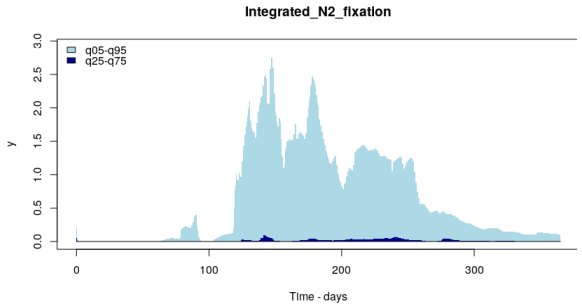

Figure 3.40: **Global sensitivity on nitrogen fixation - NFP**

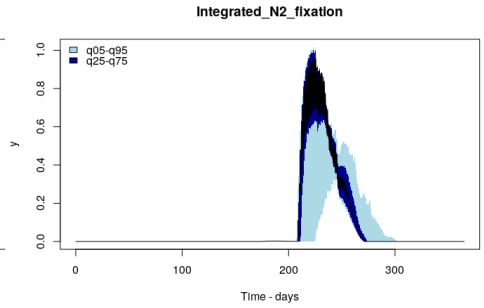

Figure 3.41: **Global sensitivity on nitrogen fixation - CP**

These two graphs point out the differences in response to variations of NFP and CP parameters with respect to N_2 fixation. As what could be expected, the model reacts much more

[3]half saturation constant of light intensity

following a change in NFP parameters. The global sensitivity to N_2 fixation shows that there are huge uncertainties in the results. The rates found by the model are maximum 0,07 mmol N m^{-2} d^{-1} , more than ten times smaller that what is found when the values of the parameters change in a range of 60% of their initial values.

Anammox reaction - Denitrification

The local sensitivity performed on chemical parameters shows that a small variation in one parameter has little influence on the output. The two reactions have a similar response to a change in either NFP or CP parameters. On a whole, changes in parameters related to the reactions themselves have a continuous impact on the model with a maximum uncertainty observed after day 300. Modifications in NFP parameters within the same range show little impact as long as there are no diazotrophs, but lead to larger uncertainties once the bloom has begun.

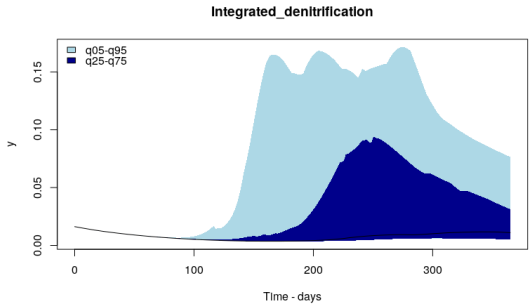

Figure 3.42: **Global sensitivity on denitrification- NFP**

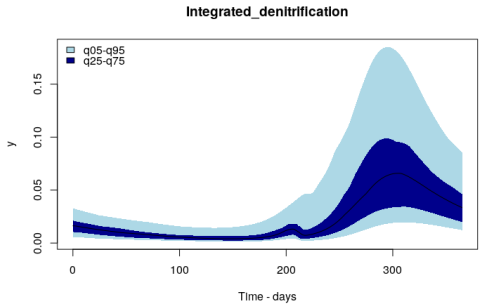

Figure 3.43: **Global sensitivity on denitrification - CP**

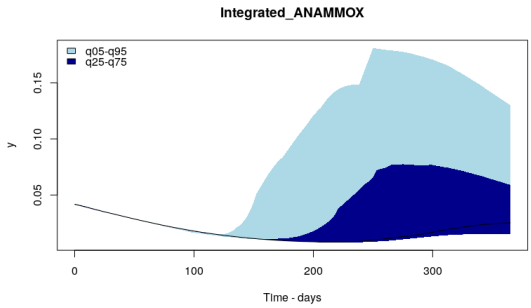

Figure 3.44: **Global sensitivity on anammox - NFP**

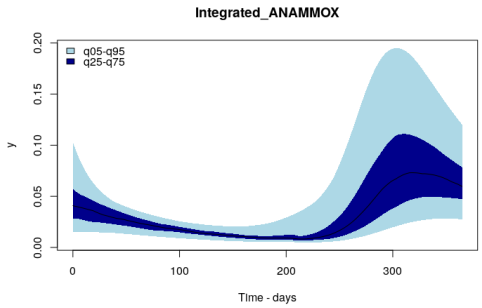

Figure 3.45: **Global sensitivity on anammox - CP**

For the parameters linked to diazotrophs, the collinearity analysis returns indexes lower than 7 for all combinations but one. The only strong relationship found is between the P:N ratio and the maximum of uptake of phosphorus (collinearity index = 168,8). Up to a combination of five

parameters, most of parameters do not present a strong connection (collinearity index less than 20).

The high sensitivity of diazotrophs on several parameters makes the modelling of this new group difficult, but its addition in the model shows that this N_2 fixation is an important reaction to take into account.

CHAPTER 4

CONCLUSION

The Black Sea is one of the well-known anoxic basins. Specific chemical reactions related to low-oxygen marine environments (i.e. denitrification, anammox) happen at an unusually low depth (typically around 100m) and over several tens of meters. Because of these reactions, 125 mmol N m^{-2} yr^{-2} ([34]) of nitrate up to 230 mmol N m^{-2} yr^{-2} ([19]) are lost for the system, depending on the model used . Meanwhile, only few measures of dinitrogen fixation rates have been made. This shows how challenging the calculation for the global nitrogen budget is in the Black Sea.

An attempt to create an additional module considering dinitrogen fixers in an existing biogeochemical model (BAMHBI[1]) is made. Up to now, the losses of fixed nitrogen (all species of nitrogen but dinitrogen) are not compensated in this model and the purpose of this project is to complete its nitrogen cycle by adding N_2 as well as dinitrogen fixers or diazotrophs.

BAMHBI, which is coupled to a physical model (NEMO[2]), is presently running in 3D in the Black Sea. Due to differences in physical forcing, the offline version in 1D requires some adjustments in respect with the 3D version before being used. In the frame of this work, the goal is to reach a reasonable solution of the years 2010's in a water column of the center of the Black Sea. The addition of a new functional group is based on the work of [45] and [35] with the necessary adaptations to be in accordance with the phytoplanktonic groups already present in BAMHBI. The new group represents a species of cyanobacteria (*Trichodesnium*) and therefore

[1]Biogeochemical Model for Hypoxic and Benthic Influenced areas

[2]Nucleus for European Modelling of the Ocean

need photosynthesis as a mean of energy. Their growth is limited by phosphorus and light but never by nitrogen. Iron is not considered as limiting. As what is described in the literature, they favor the uptake of nitrate or ammonium when available but are able to switch to N_2 as a main source of nitrogen when the two other species are lacking. An extra parameter of respiration is added taking into account the energy cost of breaking the triple bond of N_2. Grazing is not represented and diazotrophs die naturally. Dinitrogen becomes a new state variable as well and is involved in several reactions. It is created by denitrification and anammox reaction following the stoechiometric coefficients. It is removed by N_2 fixation. The air-sea flux of dinitrogen is also added in the model. At first, parameters are tuned by hand.

Even though the results are not optimal, they provide new insights on the nitrogen cycle in an peculiar environment like the Black Sea. The suggested spatial decoupling between areas of denitrification and dinitrogen fixation in the surface layer ([60]) might not be true at greater depths. Diazotrophs find a niche as deep as possible (light limitation) in the different simulations suggesting diazotrophic bacteria could thrive even deeper as suggested by a recent study by Kirkpatrick ([30]). Dinitrogen fixation seems to be an important part in the basin nitrogen cycle which is in accordance with the results of the modelling of N^*, the conservative tracer proposed by Gruber ([23]). Indeed, N^* is negative in the whole water column implying losses of fixed nitrogen. N_2 fixation could partly compensate those losses.

The next step in this project involves a sensitivity analysis of the new parameters as well as those related to denitrification and anammox. Those tests are realized with the FME packages. The results of both local and global sensitivity analyses indicate that there are large uncertainties. Given the high sensitivity of parameters regarding dinitrogen fixers, a more detailed description of this group would probably reduce part of the uncertainties.

Owing these results, it is highly possible that combining a refinement of the present work and the addition of a new group of heterotrophic diazotrophs would allow a better representation of the dinitrogen fixation in the Black Sea and lead to a better understanding of the nitrogen cycle in this part of the world.

In parallel, I also worked with NEMO 3-D to understand the basis of hydrodynamics in this model. An attempt of coupling BAMHBI and NEMO 3D in the global ocean was made, but the results are too preliminary and not yet exploitable. In the future I will use this coupled BAHMBI-NEMO-3D tool to investigate the links between the nitrogen and oxygen cycles in the global ocean.

Appendices

VARIABLES

Added variables are in bold.

Name	Group	Units
	Phytoplankton	
cfl	Flagellates	mmol C/m^3
nfl	Flagellates	mmol N/m^3
cem	Emiliana	mmol C /m^3
nem	Emiliana	mmol N /m^3
cdi	Diatoms	mmol C /m^3
ndi	Diatoms	mmol N /m^3
	Zooplankton	
mic	Micro zooplankton	mmol C /m^3
mes	Meso zooplankton	mmol C /m^3
gel	Gelatinous	mmol C /m^3
noc	Noctiluca	mmol C /m^3
	Bacteria	
bac	Bacteria	mmol C /m^3
	Diazotrophs	
cdz	Cyanobacteria	mmol C /m^3
ndz	Cyanobacteria	mmol N /m^3

Name	Group	Units
	Organic matter	
dcl	Dissolved organic carbon (labile)	mmol C /m^3
dnl	Dissolved organic nitrogen - (labile)	mmol N /m^3
dcs	Dissolved organic carbon - (semi-labile)	mmol C /m^3
dns	Dissolved organic nitrogen - (semi-labile)	mmol N /m^3
poc	Particulate organic carbon	mmol C /m^3
pon	Particulate organic nitrogen	mmol N /m^3
sid	Particulate organic silicate	mmol Si /m^3
smi	Suspended matter	gr/m^3
	Element	
nos	Nitrate and nitrite	mmol N /m^3
nhs	Ammonium and ammonia	mmol N /m^3
ntg	Nitrogen	mmol N_2 /m^3
sio	Silicate	mmol Si /m^3
dox	Oxygen	mmol O_2/m^3
dic	Dissolved inorganic carbon	mmol C /m^3
odu	Oxygen demand unit	mmol ODU /m^3
pho	Phosphate	mmol P/m^3
	Others	
agg	Aggregates	number of aggregates
CHA	charge	mmoleq-/m^3

PARAMETERS

Parameter	Units	Value	Description
	ANAMMOX		
Q10chem	-	2	Temperature coeff for chemical reactions
NOsNHsr	mol NOs (mol NHs)$^{-1}$	0.6	Mol NOs needed to oxidize one mol of NHs
kinoxnhsnos	mmol O_2 m^{-3}	8	Half-sat. const. for O_2 inhib. in NHs oxidation by NOs
kinoxnhsodu	mmol O_2 m^{-3}	0.5	Half-sat. const. for O_2 inhib. in NHs oxidation by ODU
Roxnhsnos	d$^-$1	0.05	Rate of NHs oxidation by NOs
	Denitrification		
kindenidox	mmol O_2 m^{-3}	0.5	Half-sat. const. for O_2 inhib. in denitrification
ksdeninos	mmol N m^{-3}	0.3	Half-sat. const. for NOs limitation in denitrification
NCr	mol N (mol C)$^{-1}$	0.8	Ratio Nitrogen Carbon
	Nitrification		
ksoxnhsdox	mmol O_2 m^{-3}	3.00	Half-sat. const. for O_2 limit. in NHs oxid. by O_2
Roxnhs	d$^-$1	0.03	Rate of NHs oxidation by O_2
ONoxnhsr	mol O_2 (mol NHs)$^{-1}$	2	Mol O_2 needed to oxidize one mol of NHs
	Diazotrophs		
Q10Diaz	-	1.6	Temperature coefficient
MaxNCrDiazotrophs	mol N mol C^{-1}	0.2	Maximal N:C ratio
MinNCrDiazotrophs	mol N mol C^{-1}	0.1	Minimal N:C ratio
MinChlNrDiazotrophs	g Chl mol N^{-1}	0.64	Minimal Chl:N ratio
MaxChlNrDiazotrophs	Chl mol N^{-1}	1.29	Maximal Chl:N ratio
NosMaxUptakeDiazotrophs	mol N mol C^{-1} d^{-1}	1	Max NOs uptake rate
ksNOsDiazotrophs	mmol N m^3	1	Half-sat. constant for NOs uptake
NHsMaxUptakeDiazotrophs	mol N mol C^{-1} d^{-1}	1.5	Max NHs uptake rate
ksNHsDiazotrophs	mmol N m^3	0.7	Half-sat. constant for NHs uptake
PO4MaxUptakeDiazotrophs	mol P mol C^{-1} d^{-1}	0.06250	Max PHO uptake rate
ksPO4Diazotrophs	mmol P m^{-3}	2.2	Half-sat. constant for PHO uptake
αPIDiazotrophs	d^{-1}	2	Half saturation light intensity
μMaxDiazotrophs	d^{-1}	2	Maximal growth rate
RespirationDiazotrophs	d^{-1}	0.009	Basal respiration rate
PNRedfieldDiaz	mol P mol N^{-1}	0.0625	P:N ratio according to Redfield
GrowthRespDiazotrophs	-	0.1	Part of primary production used for respiration
MortalityDiazotrophs	d^{-1}	0.095	Mortality rate
DFixDiaz	mol C mol N^{-1}	0.12	Additional respiration when N_2 fixation
bbdztShort	-	0.000007	Attenuation coefficient short wavelength diaz
bbdztL ong	-	0.000005	Attenuation coefficient long wavelength diaz

EQUATIONS

Diazotrophs evolution

$$\frac{dCDZ}{dt} = \frac{\partial}{\partial z}(\tilde{\lambda}\frac{\partial CDZ}{\partial z}) + NetPhotosynthesis - (Respiration_{\mathrm{N_2}fixation} * DFixDiaz) - CMortality - CLeakage$$

$$\frac{dNDZ}{dt} = \frac{\partial}{\partial z}(\tilde{\lambda}\frac{\partial NDZ}{\partial z}) + (\mathrm{NO_s}^{\mathrm{uptake}} + \mathrm{NH_s}^{\mathrm{uptake}} + \mathrm{N_2}^{\mathrm{uptake}}) - NMortality - NLeakage$$

Nutrient uptake if $\mathrm{NH_s}^{\mathrm{uptake}} + \mathrm{NO_s}^{\mathrm{uptake}} > \frac{\mathrm{P}^{\mathrm{uptake}}}{PNRedfield_{diaz}}$,
$\mathrm{N_2}^{\mathrm{uptake}} = 0$, otherwise :

$$\mathrm{NO_s}^{\mathrm{uptake}} = \mathrm{NO}umax * f^T * (1 - \frac{N:C}{(N:C)_{max}})\frac{\mathrm{NO_s}}{\mathrm{NO_s} + k_{\mathrm{NO_s}}}\frac{k_{in}}{k_{in} + \mathrm{NH_s}}CDZ$$

$$\mathrm{NH_s}^{\mathrm{uptake}} = \mathrm{NH}umax * f^T(1 - \frac{N:C}{(N:C)_{max}})\frac{\mathrm{NH_s}}{\mathrm{NH_s} + k_{\mathrm{NH_s}}}CDZ$$

$$\mathrm{PO_4}^{\mathrm{uptake}} = \mathrm{P}umax * f^T(1 - \frac{P:C}{(P:C)_{max}})\frac{\mathrm{P}}{\mathrm{P} + k_{\mathrm{P}}}CDZ$$

$$\mathrm{N_2}^{\mathrm{uptake}} = \frac{1}{2}(\frac{\mathrm{P}^{\mathrm{uptake}}}{PNRedfield_{diaz}} - (\mathrm{NH_s}^{\mathrm{uptake}} + \mathrm{NO_s}^{\mathrm{uptake}}))$$

for $\mathrm{NH_s}^{\mathrm{uptake}} + \mathrm{NO_s}^{\mathrm{uptake}} \geqslant \mathrm{P}^{\mathrm{uptake}} PNRedfield_{diaz}$

$$\mathrm{NO_s}^{\mathrm{uptake}} = \mathrm{NO}umax f^T * (1 - \frac{N:C}{(N:C)_{max}})\frac{\mathrm{NO_s}}{\mathrm{NO_s} + k_{\mathrm{NO_s}}}\frac{k_{in}}{k_{in} + \mathrm{NH_s}}CDZ$$

$$\mathrm{NH_s}^{\mathrm{uptake}} = \mathrm{NH}umax f^T(1 - \frac{N:C}{(N:C)_{max}})\frac{\mathrm{NH_s}}{\mathrm{NH_s} + k_{\mathrm{NH_s}}}CDZ$$

$$\mathrm{P}^{\mathrm{uptake}} = \mathrm{P}umax f^T(1 - \frac{N:C}{(N:C)_{max}})\frac{\mathrm{P}}{\mathrm{P} + k_{\mathrm{P}}}CDZ$$

$$\mathrm{N_2}^{\mathrm{uptake}} = 0$$

Temperature

$$f^T = Q_{10}^{\frac{t-20}{10}}$$

Air-sea nitrogen flux

$$AirSeaNitrogenFlux = PistonVelocity((\frac{0,78}{22.41480,000001})(SolubilityN_2) - SurfaceN_2)$$

$$PistonVelocity = \frac{0.251 * wind^2}{\sqrt{\frac{Schmidt}{600}}} \frac{86400}{360000}$$

$$Schmidt = 2304.8 - 162.75 * T + 6.2557 * T^2 - 0.013129 * T^3 + 0.00112558T^4$$

$$SolubilityN_2 = exp(-59.6274 + 85.7661\frac{100}{T} + 24.3696 * log(\frac{T}{100}))$$

$$+ salinity(-0.051580 + 0.026329(\frac{T}{100}) - 0.0037252(\frac{T}{100})^2$$

MODEL WITHOUT DIAZOTROPHS

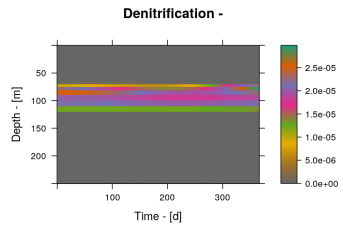

Figure 1: **Denitrification (mmolN m^{-3})**

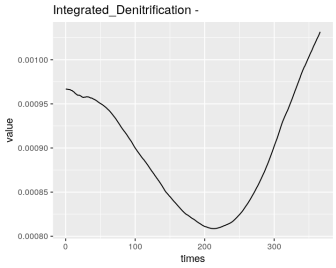

Figure 2: **Denitrification integrated (mmol N $m^{-2}d^{-1}$)**

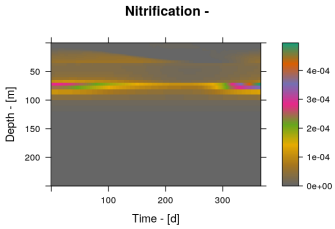

Figure 3: **Nitrification (mmolN m^{-3})**

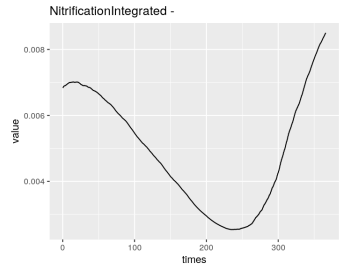

Figure 4: **Nitrification integrated (mmol N $m^{-2}d^{-1}$)**

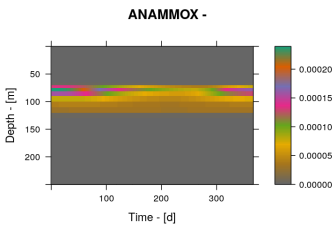

Figure 5: **Anammox (mmolN m^{-3})**

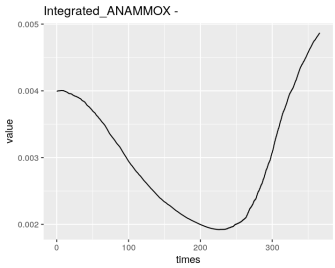

Figure 6: **Anammox integrated (mmol N $m^{-2}d^{-1}$)**

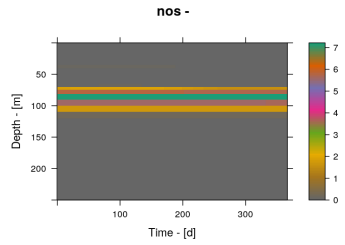

Figure 7: **Nitrate (mmolN m^{-3})**

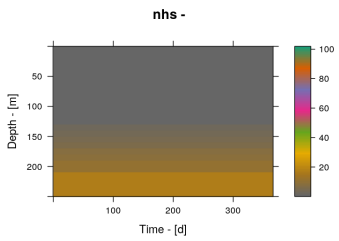

Figure 8: **Ammonium (mmol N m^{-3})**

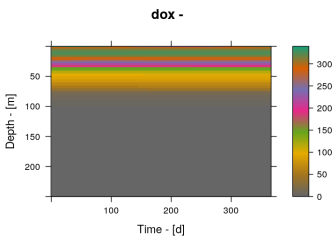

Figure 9: **Oxygen (mmol O_2 m^{-3})**

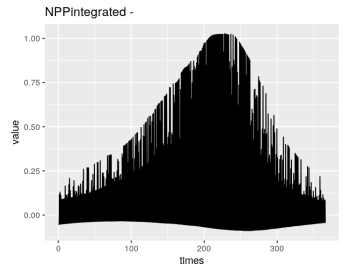

Figure 10: **Net Primary Production integrated (mmol C/m^2 d^{-1})**

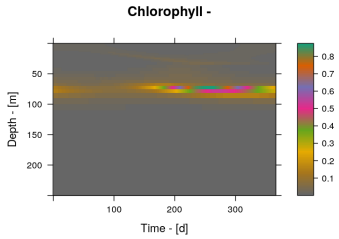

Figure 11: **Chlorophyll (mg Chl m^{-3})**

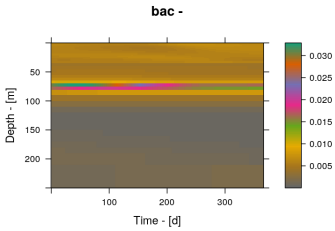

Figure 12: **Bacteria (mmol C m^{-3})**

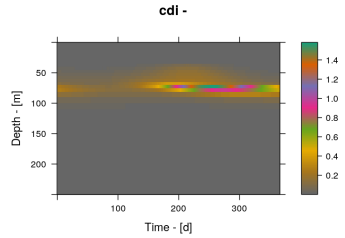

Figure 13: **Diatoms (mmol C m^{-3})**

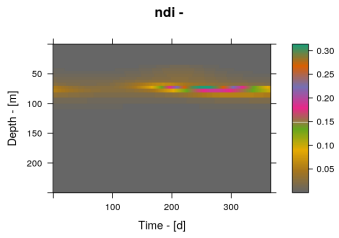

Figure 14: **Diatoms (mmol N m^{-3})**

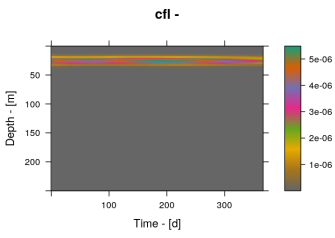

Figure 15: **Flagellates (mmol C m^{-3})**

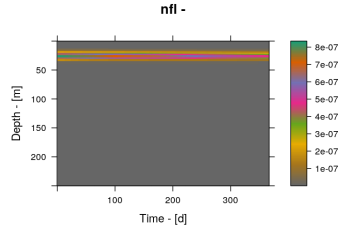

Figure 16: **Flagellates (mmol N m^{-3})**

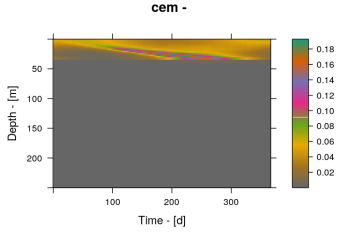

Figure 17: **Emiliana (mmol C m^{-3})**

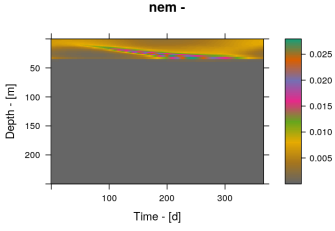

Figure 18: **Emiliana (mmol N m^{-3})**

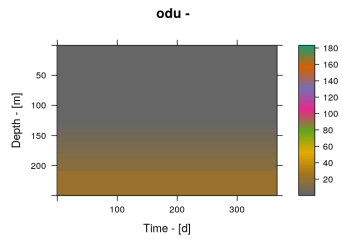

Figure 19: **ODU (mmol ODU m^{-3})**

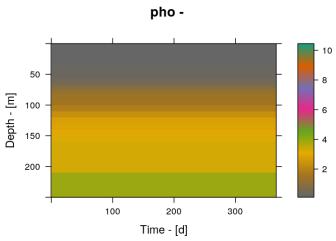

Figure 20: **Phosphate (mmol P m^{-3})**

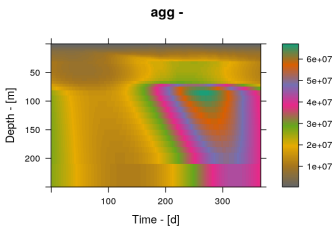

Figure 21: **Aggregates (number of agg)**

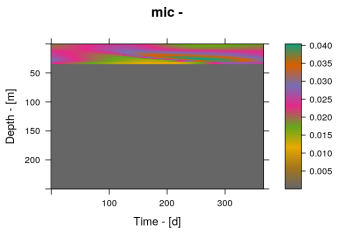

Figure 22: **Microzooplankton (mmol C m^{-3})**

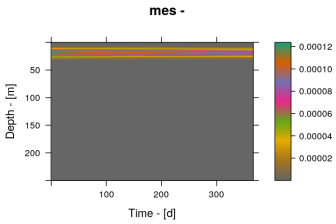

Figure 23: Mesozooplankton (mmol C m^{-3})

MODEL WITH DIAZOTROPHS

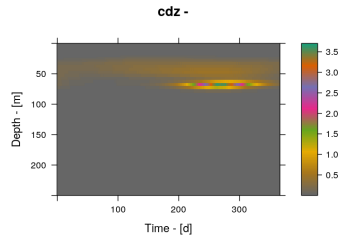

Figure 24: **Diazotrophs (mmolC m^{-3})**

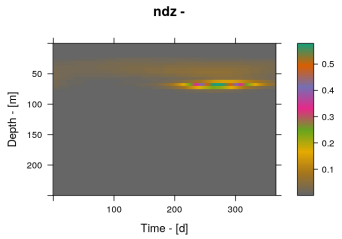

Figure 25: **Diazotrophs (mmol N $m^{-2}d^{-1}$)**

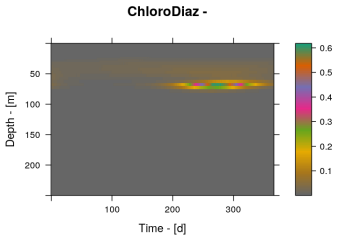

Figure 26: **Chlorophyll diaz (mg Chl m^{-3})**

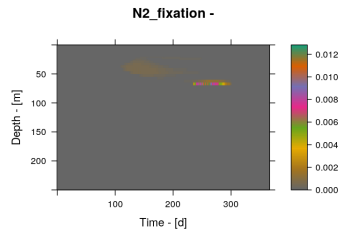

Figure 27: **N_2 fixation (mmol N $m^{-3}d^{-1}$)**

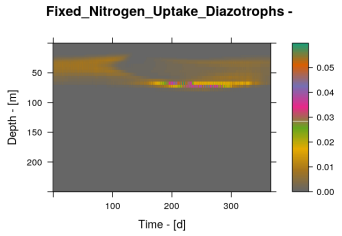

Figure 28: **Fixed N uptake (mmol N $m^{-3}d^{-1}$)**

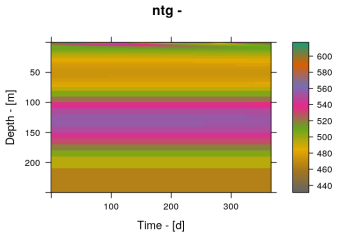

Figure 29: **Nitrogen ($mmolN_2$ m^{-3})**

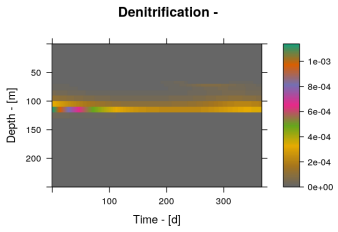

Figure 30: **Denitrification (mmolN $m^{-3}d^{-1}$)**

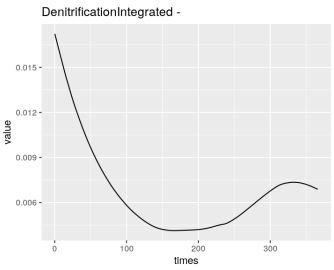

Figure 31: **Denitrification integrated (mmol N $m^{-2}d^{-1}$)**

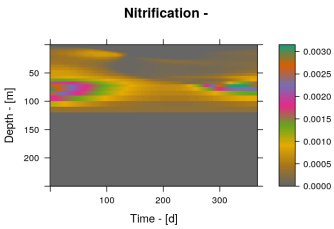

Figure 32: **Nitrification (mmolN $m^{-3}d^{-1}$)**

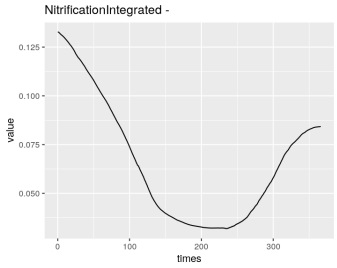

Figure 33: **Nitrification integrated (mmol N $m^{-2}d^{-1}$)**

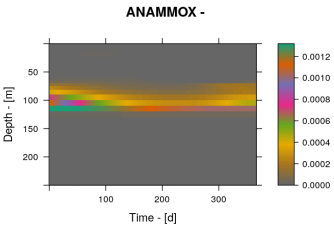

Figure 34: **Anammox (mmolN $m^{-3}d^{-1}$)**

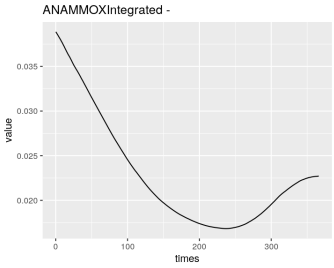

Figure 35: **Anammox integrated (mmol N $m^{-2}d^{-1}$)**

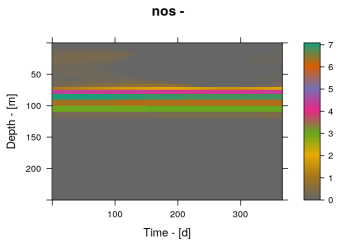

Figure 36: **Nitrate (mmolN m^{-3})**

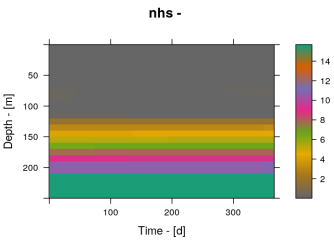

Figure 37: **Ammonium (mmol N m^{-3})**

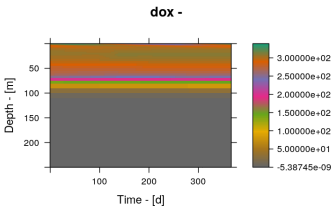

Figure 38: **Oxygen (mmol O_2 m^{-3})**

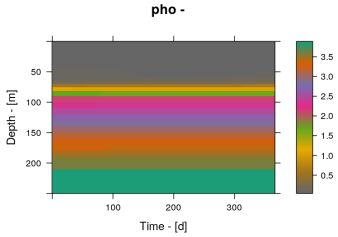

Figure 39: **Phosphate (mmol P m^{-3})**

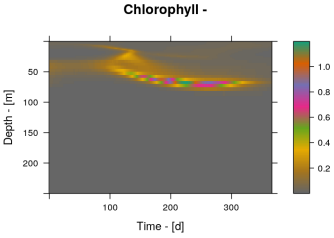

Figure 40: **Chlorophyll (mg Chl m^{-3})**

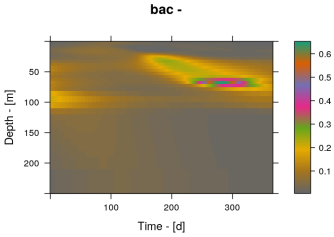

Figure 41: **Bacteria (mmol C m^{-3})**

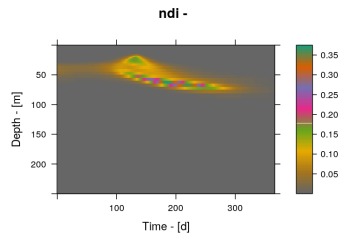

Figure 42: **Diatoms (mmol N m^{-3})**

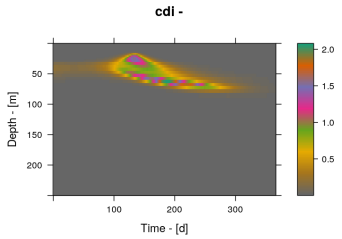

Figure 43: **Diatoms (mmol C m^{-3})**

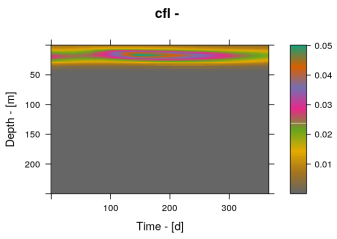

Figure 44: **Flagellates (mmol C m^{-3})**

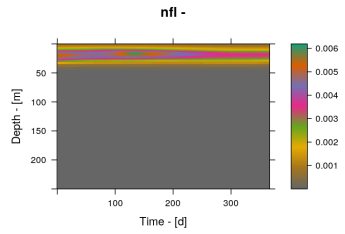

Figure 45: **Flagellates (mmol N m^{-3})**

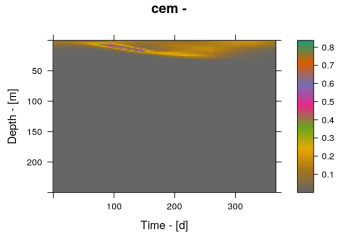

Figure 46: **Emiliana (mmol C m^{-3})**

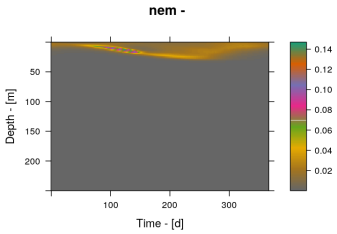

Figure 47: **Emiliana (mmol N m^{-3})**

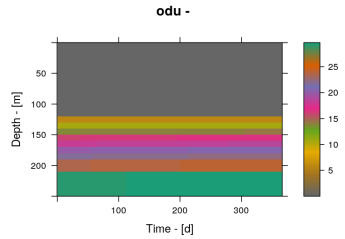

Figure 48: **ODU (mmol ODU m^{-3})**

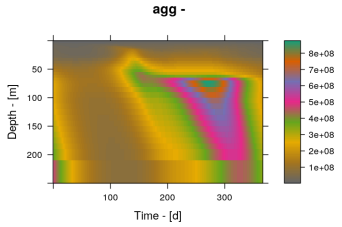

Figure 49: **Aggregates (number of agg)**

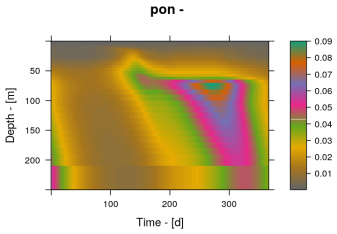

Figure 50: **Particulte organic nitrogen (mmol N m^{-3})**

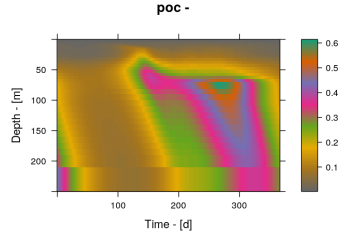

Figure 51: **Particulte organic carbon (mmol C m^{-3})**

SENSITIVITY

Parameter diaz	Chemical parameter	Variable	Diagnostic
N:Cr Diazs min and max	NOsNHsr	Oxygen	Chlorophyll Diaz
Chl:Nr Diazs min and max	kinoxnhsnox	Nitrate	ANAMMOX
MortalityDiazs	Roxnhsnos	Ammonium	Denitrification
DFix diaz	kinoxnhsodu	Dinitrogen	Nitrification
ksNHsDiazs	Q10chem	Biomass C Diazs	N2 fixation
NHsMaxUptakeDiazs	ksoxnhsdox		Maxi NHS (quantity and depth)
ksPO4Diazs	Roxnhs		Maxi chlorophyll
PO4MaxUptakeDiazs	ONoxnhsr		Maxi DOX (quantity and depth)
ksNOsDiazs	ksdeninos		Maxi NOS (quantity and depth)
NosMaxUptakeDiazs	kindenidox		Integrated Upper N Budget
bb dzt short			NPP total
bb dzt long			Integrated Upper fixed N Budget
MuMaxDiazs			Fixed N uptake by diaz
alphaPIDiazs			
GrowthRespDiazs			
Q10Diaz			
RespirationDiazs			
PNRedfieldDiaz			

Table 1: **Table 1 : Tested parameters for diazotrophs and diagnoses**

BIBLIOGRAPHY

[1] Lionel Arteaga, Markus Pahlow, and Andreas Oschlies. “Modeled Chl: C ratio and derived estimates of phytoplankton carbon biomass and its contribution to total particulate organic carbon in the global surface ocean”. In: *Global Biogeochemical Cycles* 30.12 (2016), pp. 1791–1810.

[2] D. Breitburg, M. Grégoire, and Global Ocean Oxygen Network 2018. Isensee K. (eds.) *The ocean is losing its breath: Declining oxygen in the world’s ocean and coastal waters.* Tech. rep. IOC Technical Series, No. 137 40pp. IOC-UNESCO, 2018.

[3] Cristiana Callieri et al. “The mesopelagic anoxic Black Sea as an unexpected habitat for Synechococcus challenges our understanding of global “deep red fluorescence””. In: *The ISME journal* 13.7 (2019), p. 1676.

[4] Donald E Canfield, Alexander N Glazer, and Paul G Falkowski. “The evolution and future of Earth’s nitrogen cycle”. In: *science* 330.6001 (2010), pp. 192–196.

[5] Arthur Capet et al. “Decline of the Black Sea oxygen inventory”. In: *Biogeosciences* 13 (2016), pp. 1287–1297.

[6] Arthur Capet et al. “Integrating sediment biogeochemistry into 3D oceanic models: a study of benthic-pelagic coupling in the Black Sea”. In: *Ocean Modelling* 101 (2016), pp. 83–100.

[7] Augustine T Chan. “Comparative physiological study of marine diatoms and dinoflagellates in relation to irradiance and cell size. II. Relationship between photosynthesis,

growth, and carbon/chlorophyll a ratio 1, 2". In: *Journal of phycology* 16.3 (1980), pp. 428–432.

[8] Tanya Churilova et al. "Light Absorption by Phytoplankton in the Upper Mixed Layer of the Black Sea: seasonality and Parametrization". In: *Frontiers in Marine Science* 4 (2017), p. 90. DOI: 10.3389/fmars.2017.00090.

[9] T. Churilova et al. "Phytoplankton light absorption in the deep chlorophyll maximum layer of the Black Sea". In: *European Journal of Remote Sensing* 52.sup1 (2019), pp. 123–136. DOI: 10.1080/22797254.2018.1533389.

[10] Curtis Deutsch et al. "Climate-forced variability of ocean hypoxia". In: *science* 333 (2011), pp. 336–339.

[11] Curtis Deutsch et al. "Spatial coupling of nitrogen inputs and losses in the ocean". In: *Nature* 445.7124 (2007), p. 163.

[12] C. Deutsch et al. "Denitrification and N_2 fixation in the Pacific Ocean". In: *Global Biogeochemical Cycles* 15 (2001), pp. 483–506.

[13] Yassir A Eddebbar et al. "Impacts of ENSO on air-sea oxygen exchange: Observations and mechanisms". In: *Global Biogeochemical Cycles* 31 (2017), pp. 901–921.

[14] Camila Fernandez, Laura Farias, and Osvaldo Ulloa. "Nitrogen fixation in denitrified marine waters". In: *PloS one* 6.6 (2011), e20539.

[15] Clara A Fuchsman, James W Murray, and Sergey K Konovalov. "Concentration and natural stable isotope profiles of nitrogen species in theBlack Sea". In: *Marine Chemistry* 111.1-2 (2008), pp. 90–105.

[16] Clara A. Fuchsman et al. "Detection of transient denitrification during a high organic matter event in the Black Sea". In: *Global Biogeochemical Cycles* 33 (2019).

[17] Brian T Glazer et al. "Documenting the suboxic zone of the Black Sea via high-resolution real-time redox profiling". In: *Deep Sea Research Part II: Topical Studies in Oceanography* 53.17-19 (2006), pp. 1740–1755.

[18] Marilaure Gregoire, Caroline Raick, and Karline Soetaert. "Numerical modeling of the central Black Sea ecosystem functioning during the eutrophication phase". In: *Progress in Oceanography* 76.3 (2008), pp. 286–333.

[19] Marilaure Gregoire and Karline Soetaert. “Carbon, nitrogen, oxygen and sulfide budgets in the Black Sea: A biogeochemical model of the whole water column coupling the oxic and anoxic parts”. In: *Ecological Modelling* 221 (2010), pp. 2287–2301.

[20] Nicolas Gruber. “Chapter 1 - The Marine Nitrogen Cycle: Overview and Challenges”. In: *Nitrogen in the Marine Environment (Second Edition)*. Ed. by Douglas G Capone et al. Academic Press, 2008, pp. 1–50.

[21] Nicolas Gruber. “Elusive marine nitrogen fixation”. In: *Proceedings of the National Academy of Sciences* 113.16 (2016), pp. 4246–4248.

[22] Nicolas Gruber and James N. Galloway. “An Earth-system perspective of the global nitrogen cycle”. In: *Nature* 451.7176 (2008), pp. 293–296.

[23] Nicolas Gruber and Jorge L Sarmiento. “Global patterns of marine nitrogen fixation and denitrification”. In: *Global Biogeochemical Cycles* 11 (1997), pp. 235–266.

[24] M Hannig et al. “Shift from denitrification to anammox after inflow events in the central Baltic Sea”. In: *Limnology and Oceanography* 52.4 (2007), pp. 1336–1345.

[25] Raleigh R Hood, Victoria J Coles, and Douglas G Capone. “Modeling the distribution of Trichodesmium and nitrogen fixation in the Atlantic Ocean”. In: *Journal of Geophysical Research: Oceans* 109.C6 (2004).

[26] Marlene M Jensen et al. “Rates and regulation of anaerobic ammonium oxidation and denitrification in the Black Sea”. In: *Limnology and Oceanography* 53.1 (2008), pp. 23–36.

[27] Tim Kalvelage et al. “Nitrogen cycling driven by organic matter export in the South Pacific oxygen minimum zone”. In: *Nature geoscience* 6 (2013), p. 228.

[28] Ralph F. Keeling, Arne Kortzinger, and Nicolas Gruber. “Ocean Deoxygenation in a Warming World”. In: *Annual Review of Marine Science* 2.1 (2010), pp. 199–229.

[29] John B Kirkpatrick et al. “Concurrent activity of anammox and denitrifying bacteria in the Black Sea”. In: *Frontiers in microbiology* 3 (2012), p. 256.

[30] John B Kirkpatrick et al. “Dark N2 fixation: nifH expression in the redoxcline of the Black Sea”. In: *Aquatic Microbial Ecology* 82.1 (2018), pp. 43–58.

[31] John Kirkpatrick et al. “Diversity and distribution of Planctomycetes and related bacteria in the suboxic zone of the Black Sea”. In: *Applied and environmental microbiology* 72 (2006), pp. 3079–3083.

[32] Angela N Knapp et al. “Low rates of nitrogen fixation in eastern tropical South Pacific surface waters”. In: *Proceedings of the National Academy of Sciences* 113.16 (2016), pp. 4398–4403.

[33] SK Konovalov et al. “Modeling the distribution of nitrogen species and isotopes in the water column of the Black Sea”. In: *Marine Chemistry* 111.1-2 (2008).

[34] SK Konovalov et al. “Processes controlling the redox budget for the oxic/anoxic water column of the Black Sea”. In: *Deep Sea Research Part II: Topical Studies in Oceanography* 53.17-19 (2006), pp. 1817–1841.

[35] Angela M Kuhn, Katja Fennel, and Ilana Berman-Frank. “Modelling the biogeochemical effects of heterotrophic and autotrophic N 2 fixation in the Gulf of Aqaba (Israel), Red Sea”. In: *Biogeosciences* 15.24 (2018), pp. 7379–7401.

[36] Marcel MM Kuypers et al. “Anaerobic ammonium oxidation by anammox bacteria in the Black Sea”. In: *Nature* 422 (2003), p. 608.

[37] Phyllis Lam et al. “Linking crenarchaeal and bacterial nitrification to anammox in the Black Sea”. In: *Proceedings of the National Academy of Sciences* 104.17 (2007), pp. 7104–7109.

[38] Angela Landolfi et al. “Global Marine N2 Fixation Estimates: from Observations to Models”. In: *Frontiers in microbiology* 9 (2018).

[39] Luminita Lazar et al. “Western Black Sea eutrophication status according to Black Sea eutrophication assesment tool, BEAST – MISIS cruise results”. In: *Cercetari Marine* Nr. 46 (2015), p. 48.

[40] Xin Liu et al. “Uncoupling of seasonal variations between phytoplankton chlorophyll a and production in the East China Sea”. In: *Journal of Geophysical Research: Biogeosciences* (2019).

[41] James J McCarthy et al. “Nitrogen cycling in the offshore waters of the Black Sea”. In: *Estuarine, Coastal and Shelf Science* 74.3 (2007), pp. 493–514.

[42] Svetla Miladinova et al. “Formation and changes of the Black Sea cold intermediate layer”. In: *Progress In Oceanography* 167 (July 2018), pp. 11–23.

[43] Joseph P Montoya et al. “A Simple, High-Precision, High-Sensitivity Tracer Assay for N (inf2) Fixation.” In: *Appl. Environ. Microbiol.* 62.3 (1996), pp. 986–993.

[44] Markus Pahlow, Heiner Dietze, and Andreas Oschlies. “Optimality-based model of phytoplankton growth and diazotrophy”. In: *Marine Ecology Progress Series* 489 (2013), pp. 1–16.

[45] Hanna Paulsen et al. “Incorporating a prognostic representation of marine nitrogen fixers into the global ocean biogeochemical model HAMOCC”. In: *Journal of Advances in Modeling Earth Systems* 9.1 (2017), pp. 438–464.

[46] Mercedes de la Paz et al. “Ventilation versus biology: What is the controlling mechanism of nitrous oxide distribution in the North Atlantic?” In: *Global Biogeochemical Cycles* 31.4 (2017), pp. 745–760.

[47] Sophie Rabouille et al. “Modeling the dynamic regulation of nitrogen fixation in the cyanobacterium Trichodesmium sp.” In: *Appl. Environ. Microbiol.* 72.5 (2006), pp. 3217–3227.

[48] Florian Ricour. “Study of the Deep Chlorophyll Maximum in the Black Sea as seen from Biogeochemical Argo floats”. MA thesis. University of Liege, 2018.

[49] Shubha Sathyendranath et al. “Carbon-to-chlorophyll ratio and growth rate of phytoplankton in the sea”. In: *Marine Ecology Progress Series* 383 (2009), pp. 73–84.

[50] John G. Shepherd et al. “Ocean ventilation and deoxygenation in a warming world: Introduction and overview”. In: *Philosophical Transactions of the Royal Society A: Mathematical, Physical and Engineering Sciences* 375.2102 (2017).

[51] Elliot Sherman et al. “Temperature influence on phytoplankton community growth rates”. In: *Global Biogeochemical Cycles* 30.4 (2016), pp. 550–559.

[52] Takuhei Shiozaki et al. “Factors Regulating Nitrification in the Arctic Ocean: Potential Impact of Sea Ice Reduction and Ocean Acidification”. In: *Global Biogeochemical Cycles* (2019).

[53] Karline ER Soetaert, Thomas Petzoldt, and R Woodrow Setzer. “Solving differential equations in R: package deSolve”. In: *Journal of statistical software* 33 (2010).

[54] Karline Soetaert, Thomas Petzoldt, et al. “Inverse modelling, sensitivity and monte carlo analysis in R using package FME”. In: *Journal of Statistical Software* 33.3 (2010), pp. 1–28.

[55] James T Staley. “Probing nitrogen metabolism in the redox gradient of the Black Sea”. In: *Proceedings of the National Academy of Sciences* 104.17 (2007), pp. 6881–6882.

[56] Emil V Stanev et al. “Understanding the Dynamics of the Oxic-Anoxic Interface in the Black Sea”. In: *Geophysical Research Letters* 45.2 (2018), pp. 864–871.

[57] EV Stanev et al. “Oxygen dynamics in the Black Sea as seen by Argo profiling floats”. In: *Geophysical Research Letters* 40.12 (2013), pp. 3085–3090.

[58] JH Steele and IE Baird. “Relations between primary production, chlorophyll and particulate carbon”. In: *Limnology and Oceanography* 6.1 (1961), pp. 68–78.

[59] Luc Vandenbulke, A. Capet, and M. Grégoire. *Black Sea Production Centre BLKSEA ANALYSIS FORECAST BIO 007 009*. Copernicus Marine Environment Monitoring Service, 2018.

[60] Wei-Lei Wang et al. “Convergent estimates of marine nitrogen fixation”. In: *Nature* 566.7743 (2019), pp. 205–211.

[61] XJ Wang et al. “Regulation of phytoplankton carbon to chlorophyll ratio by light, nutrients and temperature in the Equatorial Pacific Ocean: a basin-scale model”. In: *Biogeosciences* 6.3 (2009), pp. 391–404.

[62] Rik Wanninkhof. “Relationship between wind speed and gas exchange over the ocean”. In: *Journal of Geophysical Research: Oceans* 97.C5 (1992), pp. 7373–7382.

[63] Rik Wanninkhof. “Relationship between wind speed and gas exchange over the ocean revisited”. In: *Limnology and Oceanography: Methods* 12.6 (2014), pp. 351–362.

[64] BB Ward et al. “Denitrification as the dominant nitrogen loss process in the Arabian Sea”. In: *Nature* 461.7260 (2009), p. 78.

[65] Marian B Westley et al. “Nitrous oxide cycling in the Black Sea inferred from stable isotope and isotopomer distributions”. In: *Deep Sea Research Part II: Topical Studies in Oceanography* 53.17-19 (2006), pp. 1802–1816.

[66] EV Yakushev et al. “Analysis of the water column oxic-anoxic interface in the Black and Baltic Seas with a numerical model”. In: *Marine Chemistry* 107.3 (2007), pp. 388–410. DOI: 10.1016/j.marchem.2007.06.003.

[67] EV Yakushev et al. “Vertical hydrochemical structure of the Black Sea”. In: *The Black Sea Environment*. Springer, 2007, pp. 277–307.

[68] Jonathan P Zehr and Raphael M Kudela. “Nitrogen cycle of the open ocean: from genes to ecosystems”. In: *Annual review of marine science* 3 (2011), pp. 197–225.